Drivers and Impacts of Smoldering Peat Fires in the Great Dismal Swamp

Nicholas T. Link

Thesis submitted to the faculty of the Virginia Polytechnic Institute and State University
in partial fulfillment of the requirements for the degree of

Master of Science
In
Forest Resources and Environmental Conservation

Daniel L. McLaughlin, Chair
Brian D. Strahm
Ryan D. Stewart
J. Morgan Varner

May 4th, 2022
Blacksburg, VA

Keywords: Fire, Hydrology, Peat, Invasive Species, Soil Moisture Modeling, Remote Sensing, HYDRUS 1-D, *Phragmites australis*

Drivers and Impacts of Smoldering Peat Fires in the Great Dismal Swamp

Nicholas T. Link

ABSTRACT

Peatlands are a diverse type of wetland ecosystem, characterized by high levels of soil organic matter, that provide a wide array of ecosystem services including water storage and filtration, carbon sequestration, and unique habitats. Draining peatlands degrades their resilience to future disturbances, notably including high intensity, soil-consuming fires. Peat soil fires are unique in that they can smolder vertically through the soil column, with consequences ranging from large carbon emissions to altered hydrology and dramatic shifts in vegetation communities. In this work we had two complementary objectives to understand both the drivers and impacts of smoldering fires at the Great Dismal Swamp (VA and NC, USA). First, we developed and verified a new method to model peat burn depths with readily available water level and peat hydraulic property data. Our findings suggest that drainage weakens both short- and long-term controls on peat burn depths by reducing soil moisture and by decreasing peat water holding capacity. To address the impacts of smoldering fires, we quantified the abundance of the noxious *Phragmites australis* in a large fire scar and the extent to which altered hydrology influenced its occurrence. We did so by leveraging satellite imagery, random forest models, LiDAR data, and water table observations. Our results suggest that *P. australis* is aided by a hydrologic regime generated, in part, from the combined effects of drainage and deep smoldering fires. Our conclusions from these two studies contribute to the scientific understanding of smoldering peat fires and can inform management efforts.

Drivers and Impacts of Smoldering Peat Fires in the Great Dismal Swamp

Nicholas T. Link

GENERAL AUDIENCE ABSTRACT

Peatlands are a diverse type of wetland ecosystem that have characteristically thick levels of organic-rich soil, known as peat. Peatlands are home to a variety of unique plants and animals, store large amounts of carbon, and provide water storage functions. Peatlands were historically drained to enable development and conversion to other land usages, which had many unintended consequences like increasing their risk to wildfires that consume soil organic matter. An intense peat fire can smolder down through the peat, with impacts ranging from large releases of carbon to changes in water levels and vegetation communities. In this work we had two objectives aimed at understanding the drivers and impacts of smoldering peat fires in the Great Dismal Swamp (GDS) (VA and NC, USA). First, we developed and verified a new method of modeling how deep peat fires burn by using readily available water level and soil property data. Our findings suggest that drainage weakens both the short- and long-term controls on peat fire burn depths by reducing soil moisture and by limiting the ability of peats to hold water. We also studied how water levels in a post-peat consuming fire environment influence the amount of the weedy *Phragmites australis*. We did so by using satellite imagery, elevation data, and water table observations. Results from this investigation suggest that the combined effects of drainage and deep smoldering fires help to create ideal conditions for *P. australis* invasion and establishment. Our findings from these two studies add to the scientific understanding of smoldering peat fires and may inform land management decisions.

ACKNOWLEDGEMENTS

Firstly, I would like to acknowledge and thank Dr. Daniel McLaughlin for taking me on and supporting me as a student. In life you have to walk through the doors that open for you, and I am incredibly grateful that Daniel opened the door for me. I am also indebted to my committee members, Drs. Ryan Stewart, Brian Strahm, and Morgan Varner who shaped the direction of this work and provided necessary guidance.

My work in the Dismal stands on the shoulders of students like Clay Word, Morgan Schulte, and Ray Ludwig. In that same vein, I would also like the thank my lab mates and cohort, Nick Corline, Melanie McMillan, Ryan Moore, Ben Heskett, Steph Duston, Amanda Pennino, Angela Possinger, and Tyler Weiglein. For helping in the field, I would be remiss to not mention Wade Handy and Gavriel Cambridge, both of whom made the whole thing look easy.

None of what I did would be possible without the staff of the Great Dismal Swamp National Wildlife Refuge, including Fred Wurster, Chris Lowie, and Karen Balentine. Their patience and consistent support made the swamp a little less dismal. Nate Bush of the USFWS was instrumental to the remote sensing and machine learning portion of this work, and without his help there is no third chapter. Generous support from the USFWS, National Fish and Wildlife Foundation, and the Edna Bailey Sussman Fund supported this work (and myself) for which I am very appreciative.

The love from friends and family, here in Blacksburg and scattered across the map, kept me leveled and grounded. Finally, I would like to thank Malia, who rarely misses the opportunity to challenge me into being a better version of myself.

TABLE OF CONTENTS

ABSTRACT ii

GENERAL AUDIENCE ABSTRACT iii

ACKNOWLEDGEMENTS iv

LIST OF FIGURES vii

LIST OF TABLES ix

1.0 INTRODUCTION 1

1.1 Background and Justification 1

1.2 Literature Cited 5

2.0 MODELING BURN DEPTH POTENTIAL IN DEGRADED PEAT SOILS 8

2.1 Introduction 8

2.2 Methods 11

2.2.1 Study Area 11

2.2.2 Study Sites and Peat Properties 12

2.2.3 Water Table-Based Method versus HYDRUS for Burn Depth Predictions 14

2.2.4 Simulating Burn Depth Potentials Across Sites 18

2.3 Results 19

2.3.1 Water Table-Based Method versus HYDRUS for Burn Depth Predictions 19

2.3.2 Simulating Burn Depth Potentials Across Sites 22

2.4 Discussion 27

2.4.1 Approaches to Model Burn Depth Potential 28

2.4.2 Predictions of Burn Depth Potentials Across Sites 31

2.5 Literature Cited 34

3.0 INFLUENCE OF FIRE AND DISTURBANCE-ALTERED HYDROLOGY ON THE ABUNDANCE OF Phragmites australis 40

3.1 Introduction 40

3.2 Methods 43

3.2.1 Study Area 43

3.2.2 Common Reed and Other Cover Class Identification 45

3.2.3 Relationships Between Common Reed Coverage and Environmental Variables ... 50

3.3 Results 54

3.3.1 Common Reed and Other Cover Class Identification 54

3.3.2 Relationship Between Common Reed Coverage and Environmental Variables 56

3.4 Discussion 61

3.4.1 Influence of Hydrology on Common Reed 61

3.4.2 Phragmites-Fire Feedbacks 64

3.4.3 Limitations and Future Work 65

3.5 Literature Cited 67

4.0 CONCLUSIONS 73

5.0 APPENDIX 76

LIST OF FIGURES

Figure 1: Map of the Great Dismal Swamp National Wildlife Refuge, with sample locations from Chapter 2 marked. The red outline is the Lateral West burn scar, a 2502 ha marsh whose boundaries are defined by the 2011 fire, which is the study site for Chapter 3 4

Figure 2: A) Comparison of the Upper and Lower Peat soil capillary lengths for the 11 sites. B) Comparison of the Upper and Lower Peat tension-to-ignition ($h_{tension}$, cm) values for the 11 sites at the H risk level. Specific values for Sites 2, 5 and 9 from Upper-1 and Lower-1 samples labeled where present. 15

Figure 3: A) Modeled and observed hourly water tables relative to ground surface for Site 9. B) Modeled versus observed water tables for Site 9, dashed black line is a line of best fit ($\rho = 0.93$). 19

Figure 4: Modeled water tables from HYDRUS and corresponding modeled burn depths from both HYDRUS and water table-based approaches (upper panels). No burn events from the HYDRUS approach shown in black. Difference in hourly burn depth predictions between methods (Δ_{burn}) (lower panels). Site 2 Upper K_{sat} (A), Site 5 with layer appropriate K_{sat} (B) and for Site 5 with Lower K_{sat} (C). 22

Figure 5: Burn depth potentials modeled by the water table-based method at the H risk level and observed water tables relative to ground surface across the 11 sites from April 2017 – September 2019. Total depth of Upper stratum layers shown. Lower stratum layers, where present, are truncated to 1.25 m below ground surface; Sites 1, 2 ,4, 5, & 11 had no Lower Peat present. In Site 2, the water table periodically dropped into the mineral layer. The discretization of sampled hydraulic properties is noted with horizontal lines. 24

Figure 6: Burn depth potentials across the 11 sites from April 2017 – September 2019 at the H risk level, with percentage of time at risk of burning noted above each site. 25

Figure 7: Burn depth potential at the three risk levels compared across the 11 sites for April 2017 – September 2019. 26

Figure 8: A) Relationship between the mean burn depth potential modeled by the water table based-approach for the highest risk level from April 2017 – September 2019 against mean water table position ($R^2 = 0.92$, p-value < 0.001) and B) against soil capillary length for the Upper-1 sample (Spearman's $\rho = 0.809$, p-value = 0.003). 27

Figure 9: The Lateral West burn scar with ground-truthing data point locations and classes noted. Ditches within the burn scar are shown, and Interior Ditch is labeled. 45

Figure 10: Moran's I sensitivity analysis, demonstrating the scale dependence of spatial autocorrelation from one- to ten-pixel neighborhood scales. 49

Figure 11: Schematic of a binary, pixel raster cell (2.54 m resolution), and a kernel (7.62 m resolution) and super kernel (22.86 m resolution) up-sampled from the pixel. Green and 1 denote presence, red and 0 denote absence. Kernel example is 55.5% coverage, super kernel example is 35.8% coverage. 50

Figure 12: Study site north of Interior Ditch along with well locations and the LiDAR-derived digital elevation model. 51

Figure 13: Linear regression between synchronous water table elevations at Wells 1 and 2 52

Figure 14: Map of the modeled land cover classes as produced by the supervised classification of high-resolution satellite imagery (2.54 m). White space denotes areas where no one class was confidently predicted by the models. 56

Figure 15: A) Water level distribution of presence and absence observations at the pixel resolution. B) Water level distributions for each of the kernel coverages. C) Kernel coverages vs. their mean water levels ($\rho = 0.95$). D) Water level distributions for each of the super kernel coverages. E) Super kernel coverages vs. their mean water levels ($\rho = 0.81$). 58

Figure 16: Number of presence and absence observations for the areas that burned once and twice. Areas that burned once had 3.30% present observations; areas that burned twice had 29.92% present observations. 59

Figure 17: Density plots of water levels for both burn levels. Notably, the areas that have burned twice are wetter on average (0.02 m compared to 0.14 m) and are more left skewed. 60

Figure 18: Proposed Phragmites-fire feedback. High-severity, peat-consuming fires, driven by a history of drainage, alter topography and therefore hydrology. The post-disturbance environment is primed for common reed invasion with wetter conditions and the aggressive nature of common reed allows it to outcompete other species. Other studies have shown that fires increase reed bud development and shoot density (Cowie et al., 1992; Ostendorp, 1999), and that stands are highly flammable (Thompson & Shay, 1985), so they may serve as future ignition points, thereby initiating a perpetual Phragmites-fire feedback cycle. 65

Figure A-1: *Phragmites australis* observations from a 2020 aerial survey, conducted by the US Fish and Wildlife Service. Figure courtesy of the Great Dismal Swamp National Wildlife Refuge staff of the US Fish and Wildlife Service. 76

Figure A-2: Great Dismal Swamp National Wildlife Refuge *Phragmites australis* treatment areas 2012-2013. Lateral West burn scar perimeter noted in red. Figure courtesy of the Great Dismal Swamp National Wildlife Refuge staff of the US Fish and Wildlife Service. 77

LIST OF TABLES

Table 1: Comparisons between modeled burn depth potentials from HYDRUS and water table-based methods. Reported $h_{tension}$ is only for the Upper-1 samples, and Upper Peat K_{sat} is listed for sites with multiple stratum layers. Spearman's ρ from the correlation between burn depth predictions are noted. Δ_{burn} is the difference in burn depth predictions between methods, where + Δ_{burn} denotes HYDRUS burning deeper than the water table-based method. Medians and standard deviations, in parenthesis, provided for both. Only % time at burn risk is shown for HYDRUS simulations because modeled water tables remained at depths greater than $h_{tension}$ for all sites, resulting in 100% time at burn risk for water table-based predictions. MDWP is moderately decomposed woody peat, UMP is undecomposed moss peat both from Verry et al. (2011) and FP is fen peat from Simhayov et al. (2018). 21

Table 2: Classification accuracy terms from the random forest models for both the 70:30 hold-out and the tenfold cross validation methods for each cover class. All values are percentages. Producer's accuracy is the number of correctly classified testing points divided by the total number of testing points. User's accuracy is the number of correctly classified testing points divided by the total number of points determined to be that class. TSS is the summation of the probabilities that the model correctly identifies presences and absences minus one. 54

Table 3: Regression coefficients from the three auto-logistic regression models reported as odds. Nagelkerke's R^2 values reported. 60

1.0 INTRODUCTION

1.1 BACKGROUND AND JUSTIFICATION

Peatlands are a diverse type of wetland ecosystem that are characterized by deep, organic-rich soils. Supplying a host of important ecosystem services, peatlands improve water quality, provide water storage functions, produce food and textile materials, and support a diverse array of biotic communities (Zedler & Kercher, 2005). The characteristically deep deposits of soil organic matter, known as peats, develop as net primary productivity outpaces decomposition, which is limited due to anaerobic conditions and enzymatic constraints (Limpens et al., 2008; Freeman et al., 2001). This unbalanced relationship between primary production and decomposition means that peatlands are major carbon sinks, storing approximately twice the amount of carbon as the atmosphere (USGCRP, 2018).

Despite the numerous benefits, an estimated 14.1% of peatlands in the contiguous United States were drained and degraded by the mid-1990s to enable other land uses (Joosten, 2010). The long history of drainage has limited the ability of peatlands to provide ecosystem services, while in tandem making them increasingly vulnerable to future disturbances like wildfires (Page & Baird, 2016; Poulter et al., 2006). Peatland fires differ from fires in other systems as they can smolder vertically down through the soil column (Hawbaker et al., 2016; Reardon et al., 2007), with high severity fires having been observed consuming up to two meters of peat thickness, thereby releasing large amounts of carbon (Drexler et al., 2017). Draining a peatland has obvious and immediate implications for fire risk as it lowers water tables, thereby reducing soil moisture (Reardon et al., 2007; Schulte et al., 2019). Over the long-term, sustained drainage can alter soil hydraulic properties (Schwärzel et al., 2002) in a way that may have persistent influence on the water holding capacities of peats (Word et al., 2022). The relative contributions of these two

consequences of drainage to current fire risk are not well understood. Further, methods of predicting smoldering fire severity are either overly simplified or complex, and having an accurate and efficient assessment of risk is desired by land managers and planners (Fire Environment Working Group, 2009).

An important consequence of high-severity peat fires is that they alter wetland bathymetry and thus local water level regimes, thereby changing landscape form and function (Watts & Kobziar, 2013; Watts et al., 2015), while also destroying plant regenerative material both above and below ground (Matlaga et al., 2010). All of these factors influence the species that recolonize post-fire and successional trajectories (Gorham & Rochefort, 2003). Peatland ecosystems are highly prone to invasive species generally but are especially vulnerable immediately following disturbance events (Zedler & Kercher, 2004). One species that is able to take advantage of a post-disturbance environment with high success is *Phragmites australis* (Chimner et al., 2016; Ji et al., 2009; Wilcox et al., 2003). Multiple competitive advantages, such as rapid vegetative reproduction (Marks et al., 1994) and numerous windblown seeds (Kettenring & Mock, 2012), enable *P. australis* to aggressively colonize disturbed peatlands with dense, near-monospecific stands that limit the abundance of native species (Farnsworth & Meyerson, 1999). Given the aggressive nature of *P. australis*, and its capacity to reduce habitat quality (Able & Hagan, 2003; Robichaud & Rooney, 2017), it is important that we thoroughly understand the controls on its abundance in heavily disturbed systems. This information would inform invasion ecology theory and help land managers in prevention and removal strategies.

Advancing our understanding of the controls on high severity peat fires would aid in their mitigation efforts, which would in-turn limit the susceptibility of these systems to invasive species. Averting invasions from species like *P. australis*, which given its biology may initiate a

grass-fire feedback cycle (D'Antonio & Vitousek, 1992) – where fire promotes grass invasions and highly flammable grasses provide fuel for fires – would prevent further degradation. To develop our understanding of both the drivers and impacts of smoldering peat fires, it would be beneficial to work in a peatland system that has experienced drainage, high severity fires, and *P. australis* invasion. To that end, the Great Dismal Swamp National Wildlife Refuge (GDS) is an ideal study location for these investigations (Fig. 1). GDS is a 54,000 ha, federally protected freshwater peatland that has experienced both high severity peat fires and *P. australis* invasion. Previous research efforts in GDS have collected and analyzed numerous peat samples that were co-located with water monitoring wells (Fig.1) (Word et al., 2022) and derived site-specific peat moisture-to-ignition thresholds (Schulte et al., 2019). These datasets combined present the opportunity to test a new methodology of burn depth predictions as well as an investigation of the short- and long-term impacts of drainage on fire risk. Additionally, recent deep, smoldering burns in GDS are now invaded with patches of *P. australis*. By combining high resolution satellite imagery, LiDAR-derived elevation data, and water level data, we can investigate the role that a disturbance-altered hydrology, among other site factors, may have on *P. australis* abundance in a peatland that has recently experienced high severity wildfire.

The aims of the following two chapters are to: i) develop and compare different models of peat burn depth potentials to then assess fire vulnerability across GDS and ii) map *P. australis* abundance across a portion of GDS and relate its occurrence to site parameters, namely post-fire water level regimes. These two chapters can be read as standalone pieces (holding references to Fig. 1) and have been written in the Manuscript ETD format per the Virginia Tech electronic theses and dissertations guidelines.

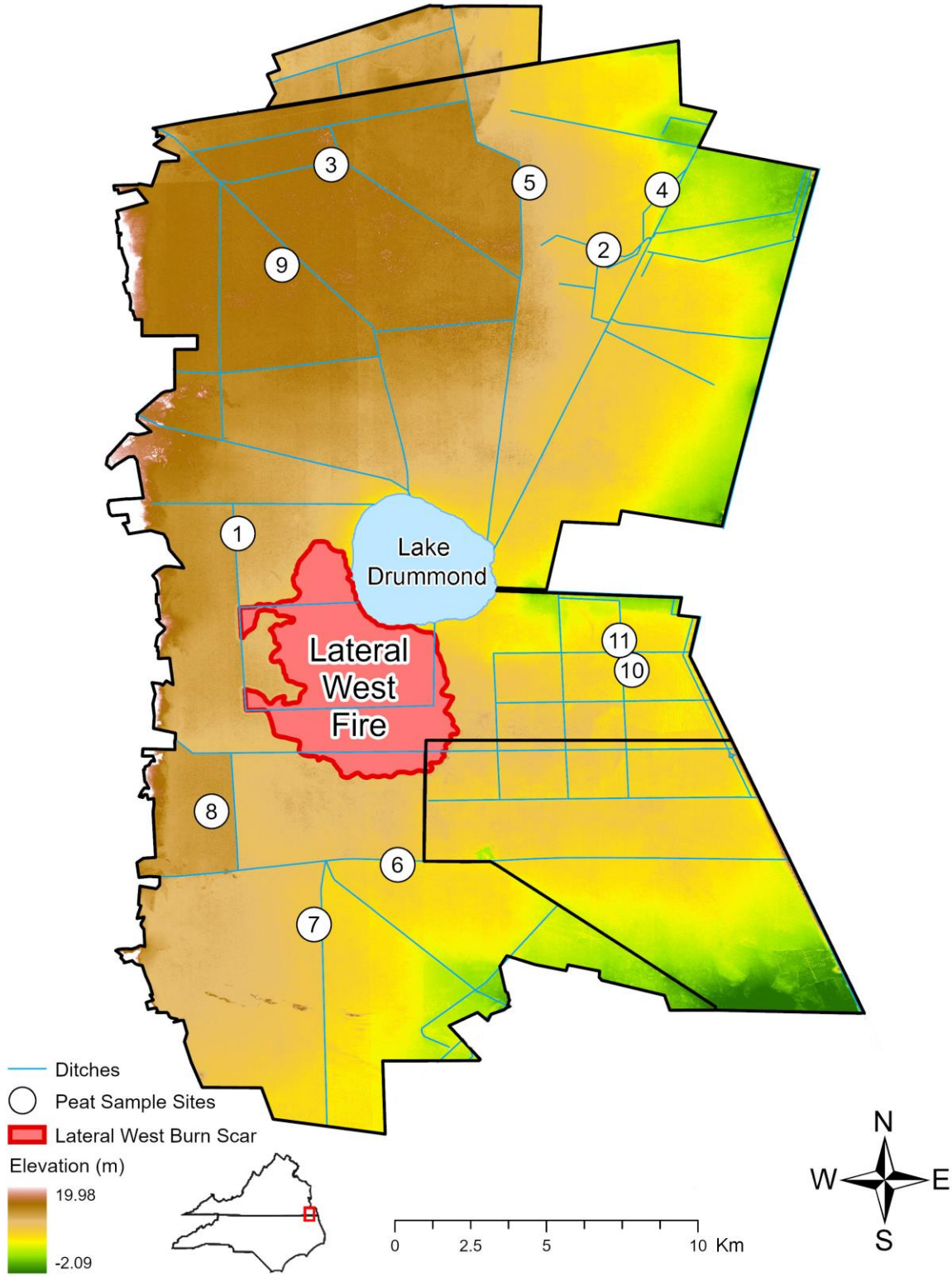

Figure 1: Map of the Great Dismal Swamp National Wildlife Refuge, with sample locations from Chapter 2 marked. The red outline is the Lateral West burn scar, a 2502 ha marsh whose boundaries are defined by the 2011 fire, which is the study site for Chapter 3.

1.2 LITERATURE CITED

Able, K. W., & Hagan, S. M. (2003). Impact of common reed, *Phragmites australis*, on essential fish habitat: Influence on reproduction, embryological development, and larval abundance of mummichog (*Fundulus heteroclitus*). Estuaries 26: 40–50. https://doi.org/10.1007/BF02691692

Chimner, R. A., Cooper, D. J., Wurster, F. C., & Rochefort, L. (2016). An overview of peatland restoration in North America: where are we after 25 years? Restoration Ecology 25: 283–292. https://doi.org/10.1111/rec.12434

D'Antonio, C. M., & Vitousek, P. M. (1992). Biological invasions by exotic grasses, the grass/fire cycle, and global change. Annual Review of Ecology and Systematics 23: 63–87. https://doi.org/10.1146/annurev.es.23.110192.000431

Drexler, J. Z., Fuller, C. C., Orlando, J., Salas, A., Wurster, F. C., & Duberstein, J. A. (2017). Estimation and uncertainty of recent carbon accumulation and vertical accretion in drained and undrained forested peatlands of the Southeastern USA. Journal of Geophysical Research: Biogeosciences 122: 2563–2579. https://doi.org/10.1002/2017JG003950

Farnsworth, E. J., & Meyerson, L. A. (1999). Species composition and inter-annual dynamics of a freshwater tidal plant community following removal of the invasive grass, *Phragmites australis*. Biological Invasions 1: 115–127. https://doi.org/10.1023/A:1010068607630

Fire Environment Working Group. (2009). Estimated smoldering potential. In 'NC Fire Effects Technical Note 01.' Raleigh, NC, USA. Available:

Freeman, C., Ostle, N., & Kang, H. (2001). An enzymic "latch" on a global carbon store: A shortage of oxygen locks up carbon in peatlands by restraining a single enzyme. Nature, 409: 149. https://doi.org/10.1038/35051650

Gorham, E., & Rochefort, L. (2003). Peatland restoration: A brief assessment with special reference to sphagnum bogs. Wetlands Ecology and Management 11: 109–119. https://doi.org/10.1023/A:1022065723511

Hawbaker, T. J., Reddy, A. D., Zhu, Z., Wurster, F. C., & Duberstein, J. A. (2016). Quantifying above and belowground carbon loss following wildfire in peatlands using repeated lidar measurements. Proceedings of the 15th International PEAT Congress, 676–680. Retrieved from http://www.peatsociety.org/document/quantifying-above-and-belowground-carbon-loss-following-wildfire-peatlands-using-repeated

Ji, Y. H., Zhou, G. S., Lv, G. H., Zhao, X. L., & Jia, Q. Y. (2009). Expansion of *Phragmites australis* in the Liaohe Delta, north-east China. Weed Research 49: 613–620. https://doi.org/10.1111/j.1365-3180.2009.00727.x

Joosten, H. (2010). The Global Peatland Carbon dioxide Picture. Wetland International. Retrieved from http://linkinghub.elsevier.com/retrieve/pii/S0277379111000333

Kettenring, K. M., & Mock, K. E. (2012). Genetic diversity, reproductive mode, and dispersal differ between the cryptic invader, *Phragmites australis*, and its native conspecific. Biological Invasions 14: 2489–2504. https://doi.org/10.1007/s10530-012-0246-5

Limpens, J., Berendse, F., Blodau, C., Canadel, J. G., Freeman, C., Holden, J., … Schaepman-Strub, G. (2008). Erratum: Peatlands and the carbon cycle: From local processes to global implications a synthesis. Biogeosciences 5, 1475-1491. https://doi.org/10.5194/bg-5-1739-2008

Marks, M., Lapin, B., & Randall John. (1994). *Phragmites australis (P. communis*): Threats, management, and monitoring. Natural Areas 14, 185–194. Matlaga, D. P., Quintana-

Ascencio, P. F., Menges, E. S., & Pickert, R. (2010). Fire mediated edge effects in bayhead tree islands. Journal of Vegetation Science 21: 190–200. https://doi.org/10.1111/j.1654-1103.2009.01132.x

Page, S., & Baird, A. J. (2016). Peatlands and global change: Response and resilience. Annual Review of Environment and Resources 41: 35–57. https://doi.org/10.1146/annurev-environ-110615-085520

Poulter, B., Christensen, N. L., & Halpin, P. N. (2006). Carbon emissions from a temperate peat fire and its relevance to interannual variability of trace atmospheric greenhouse gases. Journal of Geophysical Research 111: 1-11. https://doi.org/10.1029/2005JD006455

Reardon, J., Hungerford, R., & Ryan, K. (2007). Factors affecting sustained smouldering in organic soils from pocosin and pond pine woodland wetlands. International Journal of Wildland Fire 16: 107–118. https://doi.org/10.1071/WF06005

Robichaud, C. D., & Rooney, R. C. (2017). Long-term effects of a *Phragmites australis* invasion on birds in a Lake Erie coastal marsh. Journal of Great Lakes Research 43: 141–149. https://doi.org/10.1016/j.jglr.2017.03.018

Schulte, M. L., McLaughlin, D. L., Wurster, F. C., Varner, J. M., Stewart, R. D., Aust, W. M., … Gile, B. (2019). Short- and long-term hydrologic controls on smouldering fire in wetland soils. International Journal of Wildland Fire 28: 177–186. https://doi.org/10.1071/WF18086

Schwärzel, K., Renger, M., Sauerbrey, R., & Wessolek, G. (2002). Soil physical characteristics of peat soils. Journal of Plant Nutrition and Soil Science 165: 479–486. https://doi.org/10.1002/1522-2624(200208)165:4<479::AID-JPLN479>3.0.CO;2-8

USGCRP, 2018: Second State of the Carbon Cycle Report (SOCCR2): A Sustained Assessment Report [Cavallaro, N., G. Shrestha, R. Birdsey, M. A. Mayes, R. G. Najjar, S. C. Reed, P. Romero-Lankao, and Z. Zhu (eds.)]. U.S. Global Change Research Program, Washington, DC, USA, 878 pp., https://doi.org/10.7930/SOCCR2.2018

Watts, A. C., & Kobziar, L. N. (2013). Smoldering combustion and ground fires: Ecological effects and multi-scale significance. Fire Ecology 9: 124–132. https://doi.org/10.4996/fireecology.0901124

Watts, A. C., Schmidt, C. A., McLaughlin, D. L., & Kaplan, D. A. (2015). Hydrologic implications of smoldering fires in wetland landscapes. Freshwater Science 34: 1394–1405. https://doi.org/10.1086/683484

Wilcox, K. L., Petrie, S. A., Maynard, L. A., & Meyer, S. W. (2003). Historical distribution and abundance of *Phragmites australis* at Long Point, Lake Erie, Ontario. Journal of Great Lakes Research 29: 664–680. https://doi.org/10.1016/S0380-1330(03)70469-9

Word, C. S., McLaughlin, D. L., Strahm, B. D., Stewart, R. D., Varner, J. M., Wurster, F. C., … Link, N. T. (2022). Peatland drainage alters soil structure and water retention properties: implications for ecosystem function and management. Hydrological Processes 36: 1–12. https://doi.org/10.1002/hyp.14533

Zedler, J. B., & Kercher, S. (2004). Causes and consequences of invasive plants in wetlands: Opportunities, opportunists, and outcomes. Critical Reviews in Plant Sciences 23: 431-452. https://doi.org/10.1080/07352680490514673

Zedler, J. B., & Kercher, S. (2005). Wetland resources: Status, trends, ecosystem services, and restorability. Annual Review of Environment and Resources 30: 39–74 https://doi.org/10.1146/annurev.energy.30.050504.144248

2.0 MODELING BURN DEPTH POTENTIAL IN DEGRADED PEAT SOILS

2.1 INTRODUCTION

Peatlands are a diverse set of wetland ecosystems characterized by saturated soils and high levels of soil organic matter. Supplying a wide variety of important ecosystem services, peatlands improve water quality, provide water storage, and support a diverse array of flora and fauna (Zedler & Kercher, 2005). The deep organic soils that characterize peatlands develop as net primary productivity outpaces decomposition due to anaerobic conditions and enzymatic constraints (Limpens et al., 2008; Freeman et al., 2001). Consequently, peatlands are major carbon (C) sinks, with northern circumpolar zones alone storing 1,460 to 1,600 Pg C, or approximately twice the amount of C in the atmosphere (USGCRP, 2018). Yet, sizeable peatland extent has been drained for expanding development and agriculture since European colonization, with an estimated 14.1% of peatlands in the contiguous United States degraded by the mid-1990s (Joosten, 2010). Decades of drainage have resulted in increased soil oxidation, altered vegetation communities, and, importantly, greater fire risk (Holden et al., 2004; Paal et al., 2016; Page & Baird, 2016; Poulter et al., 2006).

Fires in peatlands are a natural process that help cycle nutrients and maintain distinct plant communities, particularly fire-adapted species (Loveless, 1959). While periodic surface fires are normal, threats to peatland resilience arise when fire severity increases. Compared to other ecosystems, fires in peatlands are unique in that they can smolder vertically down within the soil column, burning considerable quantities of organic matter (Hawbaker et al., 2016; Reardon et al., 2007). Particularly severe smoldering fires can consume up to 2 meters of peat vertically and can burn for months (Drexler et al., 2017; Sleeter et al., 2017; Turetsky et al., 2015). The deeper a peat-consuming fire burns, the larger the C emissions (Poulter et al., 2006),

meaning that high severity fires can undo centuries of C accumulation (Kuhry, 1994; Sleeter et al., 2017; Turetsky et al., 2015), greatly outweighing a system's potential for long-term sequestration (Pindilli, et al., 2018; Rein, 2015). Beyond these global C implications, high severity burns also have dramatic local impacts, where deep burns can vastly alter local topography and therefore hydrology (Watts et al., 2015). Deep burns also remove vegetation and regenerative tissue both above and below ground (Matlaga et al., 2010). As such, land managers are increasingly concerned with peatland fire prevention and prediction (Fire Environment Working Group, 2009), both of which would benefit from an improved understanding of the drivers of peat fire severity.

Intuitively, as the moisture content in a peat decreases its flammability increases (Prat-Guitart et al., 2016; Reardon et al., 2007), meaning that both the threat of ignition and depth of peat consumption are directly dependent on dynamic soil moisture regimes. Soil moisture profiles in peatlands are controlled by both hydrologic inputs and outputs as well as soil hydraulic properties, including pore structures and their influence on hydraulic conductivity and water retention. Artificially draining a peatland has clear short-term implications for flammability as it lowers water tables and reduces soil moisture (Reardon et al., 2007; Schulte et al., 2019). Yet, sustained drainage can also have long-term impacts on soil hydraulic properties (Schwärzel et al., 2002) and thus a persistent influence on soil moisture regimes and associated fire risk. Soil hydraulic properties differ between peatlands, but may also vary within a site both laterally and vertically (Benscoter et al., 2011). This variation in soil properties thus indicates that there may be similar variability in soil moisture regimes and associated smoldering fire risk among and within sites. Further, peats vary in the soil moisture threshold at which ignition and

smoldering can occur, based upon properties such as bulk density and carbon content (Frandsen, 1997).

Predicting fire risk across time and space requires site-specific knowledge of soil moisture thresholds for ignition along with soil moisture observations, or predictions thereof based on soil hydraulic properties and hydroclimatic forcing. To that end, Schulte et al. (2019) quantified site-specific soil-moisture thresholds for peat ignition and developed soil moisture release curves (MRCs), which relate tension (i.e., soil water pressure potential) to moisture content throughout the soil profile. By combining these two properties, they made temporal predictions of smoldering ignition vulnerability from water table time series. Those predictions, however, were limited to surface ignitions as they relied upon MRCs developed using surface samples. Characterizing the heterogeneity of peat properties at multiple depths would enable predictions of the moisture profile throughout the vadose zone, thereby allowing for depth of burn predictions.

The water table-based models of soil moisture made by Schulte et al. (2019) also operated under the unverified assumption that the soil water in their system was rapidly returning to a resting state (i.e., hydrostatic equilibrium). If a system is at a state of hydrostatic equilibrium, then the negative tension driven by the relative position of the water table is the only dynamic factor influencing the above soil moisture profile. That assumption may be inappropriate in systems where soil water redistribution is slow, as is the case in soils with low hydraulic conductivities (Dingman, 2015). An alternative, albeit more complex, approach to predict ignition and smoldering depth risk would be to use process-based models, such as HYDRUS-1D (Šimůnek et al., 2006), which utilize known hydraulic properties to model soil moisture redistribution and profiles based on hydrologic inputs and outputs.

Our primary objective in this study was to predict smoldering depth potential, both spatially and temporally, in a drained, temperate peatland: The Great Dismal Swamp National Wildlife Refuge, Virginia and North Carolina, USA (Fig. 1). Our goals were to build upon past work focused on surface ignition in this system (Schulte et al., 2019) to: i) compare a water table-based approach that assumes hydrostatic equilibrium for predictions of soil moisture profiles and smoldering depths to that of the process-based model HYDRUS and ii) predict smoldering depth potentials over time (April 2017 to September 2019) and across sites (n = 11) using multiple MRCs developed throughout the soil profile. Our second objective was to explore the influence that a history of drainage has on contemporary peat fire risk via changes in soil hydraulic properties. Earlier work in our study system identified a bimodal stratification of the soil profile, where drained upper layers had different pore structures and lower water retention (Word et al., 2022). Given that observation and the known site history, the goal of this objective was thus to investigate the potential long-term impact of drainage on peat fire risk.

2.2 METHODS

2.2.1 Study Area

The Great Dismal Swamp (hereafter GDS) is a palustrine, forested peatland in the coastal plain ecoregion of southeastern Virginia and northeastern North Carolina, USA (36°35’49”N, 76°29’26”W). At approximately 75,000 ha, GDS is managed by a group of federal, state, and non-governmental organization partners – the largest being the US Fish and Wildlife Service who oversee the National Wildlife Refuge (NWR) of the same name (Fig. 1). Characterized by a temperate climate, the summers are hot and humid, and the winters are mild. GDS is largely rain-fed, with a mean annual precipitation of 116.2 cm and mean annual evapotranspiration of 81.3 cm (USFWS, 2006). The 144-mile drainage ditch network that bisects GDS was first dug in the

late 18th century to lower water tables and facilitate logging operations (Eggleston et al., 2018; Hansen, 2010). Once a rich mosaic of forested wetland community types, GDS is now dominated by maple-gum forests (*Acer rubrum – Nyssa spp*.) with a less significant contribution from wetland obligates such as bald cypress (*Taxodium distichum*) and Atlantic white-cedar (*Chamaecyparis thyoides*) (Ludwig et al., 2021). Deeper water tables have also likely increased smoldering fire vulnerability, as evidenced by the 2008 South One and 2011 Lateral West wildfires, which burned 1,800 ha and 2,500 ha respectively and released a combined 1.83 Tg C (Hawbaker et al., 2016), and burned 47 cm deep on average (Reddy et al., 2015). In response, GDS NWR currently operates water control structures within the ditch network to manage water table positions and dynamics. Those efforts are aimed at supporting increased C sequestration, restoring historical forest communities, and reducing vulnerability to deep, smoldering fires (Balentine, 2020).

2.2.2 Study Sites and Peat Properties

The organic rich soils of GDS are commonly referred to as a peatland following general definitions for peatlands as wetland systems with Histosols greater than 40 cm in depth (Joosten & Clarke, 2002). Therefore, we refer to such soils found in GDS hereafter as peats. The peats of GDS have two physically distinct stratum with mineral soils underlying the lower layer and occasionally occurring at the surface (Natural Resources Conservation Service, 2017). The upper layer has lower organic and fiber matter contents, higher bulk densities, and lower water retention properties, a difference attributed to a history of drainage (Word et al., 2022).

We acquired water table data and previously determined peat properties for 11 sites across GDS (site locations indicated in Fig. 1). Water table dynamics were monitored at each site with one vented, submersible, pressure transducers (either Campbell Scientific CS 450,

Campbell Scientific, Logan, UT, USA; In-Situ Level Troll 500, In-Situ Inc., Fort Collins, CO, USA; or KPSI 500; Pressure Systems Inc., Newport News, VA, USA) that collected continuous, hourly data from April 2017 through September 2019. Previous work by Word et al. (2022) collected peat cores from each site, measuring both total thickness and thickness of each individual stratum layer (hereafter Upper and Lower Peat). Samples were analyzed to develop MRCs that relate soil moisture (as percent saturation) to matric potential, expressed as positive tension. Specific details on laboratory procedures and the development of soil MRCs can be found in Word et al. (2022) and are briefly described here. For each of the 11 sites, MRCs were developed for individual samples at the 25th, 50th and 75th depth percentiles of each observed stratum layer, with a maximum of six samples per site (i.e., Upper-1, Upper-2, Upper-3, Lower-1, Lower-2, Lower-3). In situations where a stratum layer was < 40 cm thick, a single sample at the layer midpoint (50th depth percentile) was collected. For each sample, multiple tensions were applied using the tension table approach for low tensions (< 6 kPa) and pressure plate approach for higher tensions (> 33 kPa). By relating these applied tensions to their corresponding measured soil moisture values, MRCs were developed for each sample using a modified version of the Brooks and Corey (1964) model for water retention.

We also took advantage of soil moisture content thresholds for 50% smoldering probability as previously developed for three GDS locations with organic soils (see Schulte et al. 2019 for details). These threshold values (reported as gravimetric water content) were converted to percentage of total saturation ($s_{smolder}$) to constrain the variability among sites. The three values for $s_{smolder}$ were characterized as Low, Medium, and High (L, M, H) risk levels and used in the calculations of burn depth potential for both the water table-based and HYDRUS approaches described below. The H risk level was used in the comparison between modeling approaches.

We applied these three $s_{smolder}$ values to all sites because we had information for hydraulic properties for each of our 11 sites but not 50% smoldering probability thresholds.

2.2.3 Water Table-Based Method versus HYDRUS for Burn Depth Predictions

2.2.3.1 HYDRUS

HYDRUS models a soil moisture profile by solving the Richards equation for unsaturated flow (Richards, 1931) given meteorological and soil property inputs (Šimůnek et al., 2006). To ensure that HYDRUS accurately represents soil moisture profiles in our system, we selected a single site (Site 9) to calibrate hourly modeled water table positions against corresponding water table observations. Site 9 was selected as it has an intermediate soil capillary length (here used as a singular value to quantify water retention capacity) within the Upper Peat samples (Fig. 2A). Depth-specific hydraulic properties, residual soil water content, saturated soil water content, pore size index, and bubbling pressure from Word et al. (2022) and saturated hydraulic conductivity (K_{sat}) rates from Eggleston et al. (2018) were used to model soil profiles. The profile depth matched the depth measurements for upper and lower peat at that site. The upper peat layer was evenly divided into two sections as two upper peat samples were collected for Site 9. We gathered meteorological data from a weather station located at Suffolk Executive Airport, approximately 4.5 km west of GDS NWR. In addition to hourly precipitation amounts, meteorological data were used to calculate hourly evapotranspiration rates (ET) using the Penman-Monteith (1965) equation.

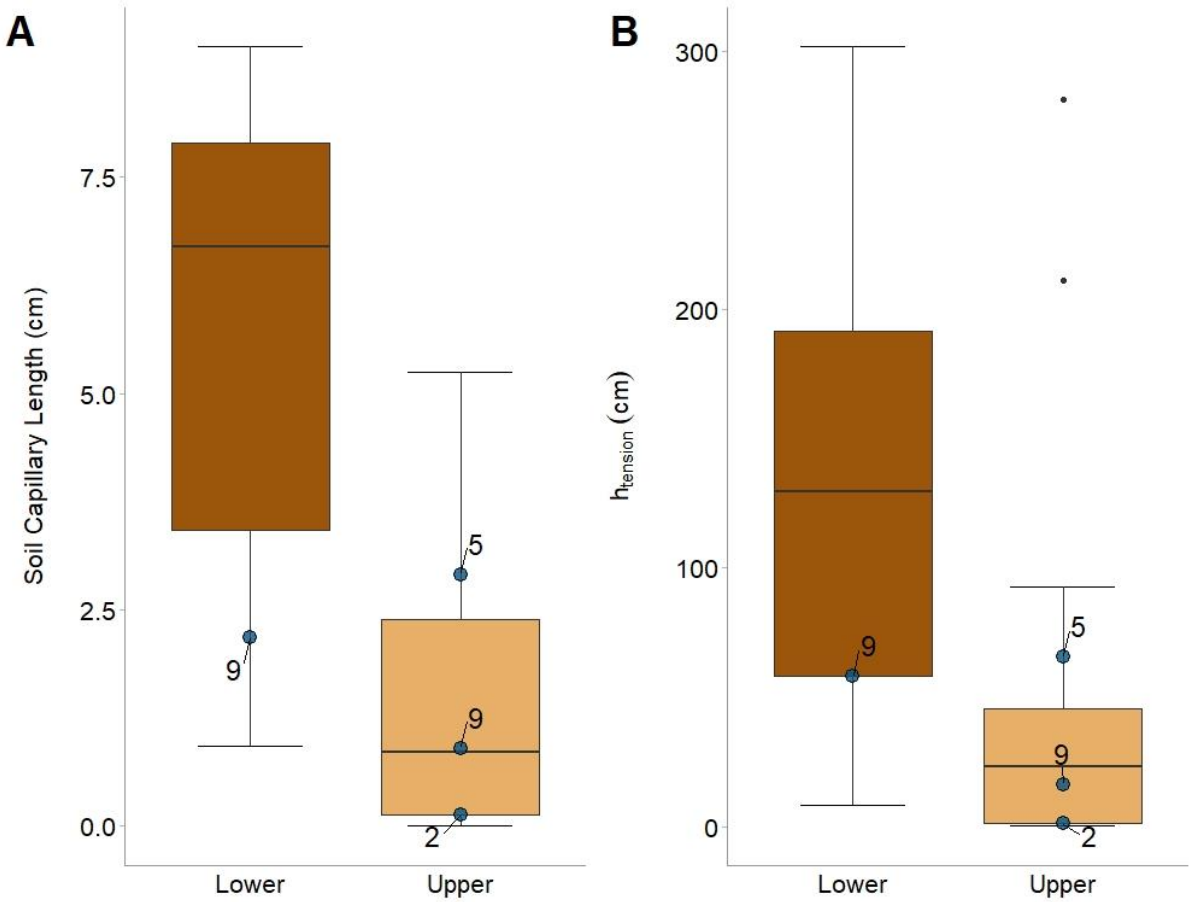

Figure 2: A) Comparison of the Upper and Lower Peat soil capillary lengths for the 11 sites. B) Comparison of the Upper and Lower Peat tension-to-ignition ($h_{tension}$, cm) values for the 11 sites at the H risk level. Specific values for Sites 2, 5 and 9 from Upper-1 and Lower-1 samples labeled where present.

Adjustments to ET were made to account for differences between potential evapotranspiration (PET) and ET via the crop coefficient method (Allen et al., 1998) and adjustments to precipitation were made to factor in losses due to canopy interception. Our calibration approach was to tune these adjustment factors in order to maximize the Spearman's rank correlation coefficient between modeled and observed water table elevations at Site 9 for a 7-week modeling period (16 June 2017 – 02 September 2017). We evaluated the final calibration factors against regionally specific measurements for both the ET to PET ratio (Shoemaker et al.,

2006; Drexler et al., 2004; German, 2000) and interception (Bryant et al., 2005) to ensure their appropriateness. These meteorological calibration factors were applied uniformly to all subsequent HYDRUS models.

Following calibration at Site 9, we generated HYDRUS models for three sites (Sites 2, 5 and 9) that represented a broad range of Upper Peat soil capillary lengths and therefore water retention properties (Fig. 2A). We focused on capturing the range in water retentions because hydraulic properties were expected to largely determine the limits of the assumption of hydrostatic equilibrium and thus the appropriateness of the water table-based approach (described below) or the necessity for the usage of HYDRUS. Additionally, the sensitivity of the HYDRUS models to K_{sat} values was explored as site specific K_{sat} values were not measured in Word et al. (2022) but rather were fitted parameters in the hydrologic models of Eggleston et al. (2018). Eggleston et al. broadly applied these values to Upper Peats (1678.9 cm/h) and Lower Peats (30.48 cm/h). We generated HYDRUS models for Sites 2, 5 and 9 with both the K_{sat} typical of their stratum position, and with the entire profile having Lower Peat K_{sat}, which allowed us to evaluate the sensitivity of our modeled profiles to variable K_{sat} rates.

To expand beyond our study system, we also generated HYDRUS models using reported hydraulic properties from three different peat types, which included a moderately decomposed woody peat (MDWP) and an undecomposed moss peat (UMP) from Verry et al. (2011) and a fen peat (FP) from Simhayov et al. (2018). All HYDRUS models were run at a 0.25 cm depth resolution (evenly discretized to reflect a site's number and depth of samples) and during the same 7-week window of meteorological data. Hourly burn depth potentials in the HYDRUS models were calculated as the shallowest point greater than the $s_{smolder}$ threshold at the H risk level.

2.2.3.2 Water Table-Based Method

For each sample at the six sites modeled in HYDRUS (Sites 2, 5, 9, MDWP, UMP, and FP), the tension (i.e., absolute value of the pressure head) required to reach the H risk level $s_{smolder}$ ($h_{tension}$, cm) was derived from their MRCs (Fig. 2B). Assuming hydrostatic equilibrium, we determined burn depth potentials as the closest height above the water table under $h_{tension}$. The soil profiles for the water table-based method models were evenly discretized to reflect the number of samples and their depths collected at each site. Burn depth potentials could not skip across sample depths (i.e. if a modeled burn did not move through the entirety of Upper-1, it could not reignite in Upper-2, even if a position in Upper-2 had a moisture content less than $s_{smolder}$).

2.2.3.3 Comparison Between Water Table-Based and HYDRUS Methods

To enable a direct comparison between the two methods, we applied the water table-based approach using the HYDRUS-simulated water tables. We used the HYDRUS-simulated water tables because Sites (2 and 5) had water table observations above ground surface for the duration of the 7-week modeling period. For this reason, initial HYDRUS-modeled water table depths had to be preset to enable depth of burn comparisons. To ensure that simulations would be under a threat of burning, we set initial water table depths equal to the initial observation depth for Site 9 or $h_{tension}$ for each site's Upper-1 sample, whichever was deeper. By taking this approach, we were able to systematically generate initial conditions for our sites and the three peats from the literature, for which we had no water table data. Hourly modeled burn depth potentials over the 7-week period from the two different approaches were compared using a Spearman's correlation analysis. We also compared the frequency of burn events between methods. Difference in hourly burn depth predictions (Δ_{burn}) were calculated to separately assess

periods when HYDRUS predicted greater (+ Δ_{burn}) or shallower burn depths (- Δ_{burn}) (see example in Fig. 4C). Results from this analysis allowed us to identify situations in which peat properties or climatic events (e.g., precipitation or periods of high evapotranspiration rates) rebuke the necessary assumption of hydrostatic equilibration for the water table-based method, thus indicating that the HYDRUS approach may be more appropriate.

2.2.4 Simulating Burn Depth Potentials Across Sites

In comparing burn depth simulations from the two approaches, we found that the hydrostatic approach is reasonable for our Upper Peats, which are characterized by low capillary potential, and therefore water retention (Fig. 2A). Thus, we applied the simpler water table-based approach across all 11 sites and three risk levels (L, M, H) to compare burn depth potentials for the entire water table record (April 2017 to September 2019). We calculated the $h_{tension}$ values for the M and L risk levels in the same way as the H risk level. Differences between risk levels at each site were evaluated to assess the impact variable $s_{smolder}$ values had on burn depth potentials. Differences among sites and risk levels at sites were assessed using non-parametric Kruskal-Wallis tests and pair-wise, post-hoc Wilcoxon rank sum tests (α= 0.05).

To better understand the factors that influence burn risk, we conducted correlation analyses (either Spearman's rank correlation and simple linear regression depending on the shape of the relationship) between site-mean burn depths and site variables. We identified surrogate variables for short- and long-term controls, specifically mean water table position for short-term and soil capillary length as an indicator for long-term. Additionally, a Spearman's rank correlation analysis was used to test for collinearity between these site variables as hydrology explained much of the variation between the hydraulic properties of peats samples in Word et al. (2022). All statistical tests and comparisons were done in R 4.0.2 (R Core Team, 2020).

2.3 RESULTS

2.3.1 Water Table-Based Method versus HYDRUS for Burn Depth Predictions

The correlation coefficient between HYDRUS-modeled and observed water tables at Site 9 for a 7-week period was maximized by setting the ratio of ET to PET set at 80% and interception loss set at 0.11 cm, (Fig. 3B, ρ = 0.93). This strong correlation provided confidence that HYDRUS applications would accurately represent the soil moisture profiles at other GDS sites. The minor disagreement between the observed and modeled values is likely due to the heterogeneity of precipitation events over such a large area, as evidenced by the mismatch of initial water table increases around the 1000 h mark and the magnitude around the 600 h mark (Fig 3A).

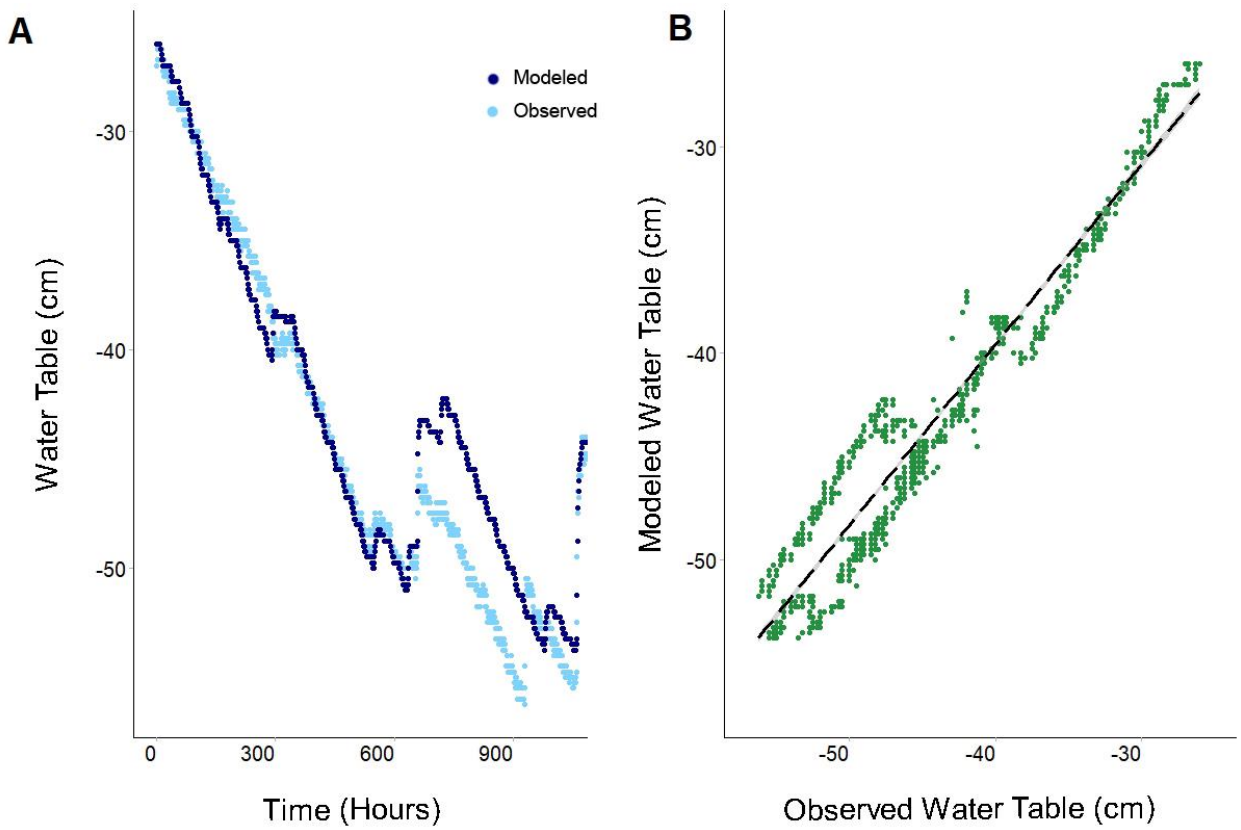

Figure 3: A) Modeled and observed hourly water tables relative to ground surface for Site 9. B) Modeled versus observed water tables for Site 9, dashed black line is a line of best fit (ρ = 0.93).

The six peats chosen for model comparison varied in their hydraulic properties – namely $h_{tension}$ and K_{sat} – with noticeable influences on the degree of divergence between water table-based and HYDRUS predictions (Δ_{burn}) and the frequency at which they were under threat of burning (Table 1, Fig. 4). When modeled with the K_{sat} rates that corresponded with their stratum layers, Sites 2, 5 and 9 all had a close agreement between methods (median +/- Δ_{burn} values < 1 cm, ρ values ≥ 0.94). The strong degree of correlation is predictable for Site 2 given its low water retention, but less expected for Sites 5 and 9, which had higher capillary lengths and thus greater water retention (Fig. 2A). Site 2 had near complete agreement between the two methods (Fig. 4A), as compared to some minor divergence at Site 5 (when applying Upper K_{sat}), which was driven by diurnal ET and precipitation events (Fig. 4B). When modeled with the K_{sat} rate reported for Lower Peat (30.48 cm/h), however, Sites 5 and 9 had much larger Δ_{burn} values than Site 2, demonstrating the varying level of influence K_{sat} had across samples that differed in water retention. This divergence is evident during drying events when HYDRUS predicts a deeper burn depth (+ Δ_{burn}), reflecting greater and sustained ET-induced soil moisture declines. It is also apparent during precipitation-induced wetting fronts where HYDRUS burn depth predictions are shallower than the water table-based approach (– Δ_{burn}) (Table 1, Fig. 4C). The influence of K_{sat} on peats with higher water retention can also be seen in MDWP, which has a low K_{sat} rate and high $h_{tension}$ value and similarly demonstrated a large degree of divergence from hydrostatic equilibrium. Despite their divergence, the separation between model predictions never exceeded 15 cm for any of the peats.

Table 1: Comparisons between modeled burn depth potentials from HYDRUS and water table-based methods. Reported $h_{tension}$ is only for the Upper-1 samples, and Upper Peat K_{sat} is listed for sites with multiple stratum layers. Spearman's ρ from the correlation between burn depth predictions are noted. Δ_{burn} is the difference in burn depth predictions between methods, where + Δ_{burn} denotes HYDRUS burning deeper than the water table-based method. Medians and standard deviations, in parenthesis, provided for both. Only % time at burn risk is shown for HYDRUS simulations because modeled water tables remained at depths greater than $h_{tension}$ for all sites, resulting in 100% time at burn risk for water table-based predictions. MDWP is moderately decomposed woody peat, UMP is undecomposed moss peat both from Verry et al. (2011) and FP is fen peat from Simhayov et al. (2018).

Peat	$h_{tension}$ (cm)	K_{sat} (cm/h)	Burn Depth ρ	+ Δ_{burn} (cm)	– Δ_{burn} (cm)	% Time at Burn Risk via HYDRUS
Site 2	1.00	1678.9	1.00	0.3 (0)	0 (0)	100
Site 2	1.00	30.48	1.00	0.3 (0)	0 (0.7)	99.7
Site 9	16.15	1678.9	0.99	0.2 (0.1)	0.1 (0.7)	99.8
Site 9	16.15	30.48	0.88	1.4 (0.5)	0.9 (4.2)	96.0
Site 5	65.66	1678.9	0.94	0.7 (0.8)	0.1 (3.1)	98.3
Site 5	65.66	30.48	0.38	13.4 (3.2)	8.3 (5.0)	90.7
MDWP	60.34	17.86	0.75	4.1 (1.6)	3.2 (6.3)	95.7
UMP	1.71	137.16	0.99	0.2 (0)	0 (0)	100
FP	84.85	106	0.92	0.6 (0.6)	0.8 (3.8)	98.1

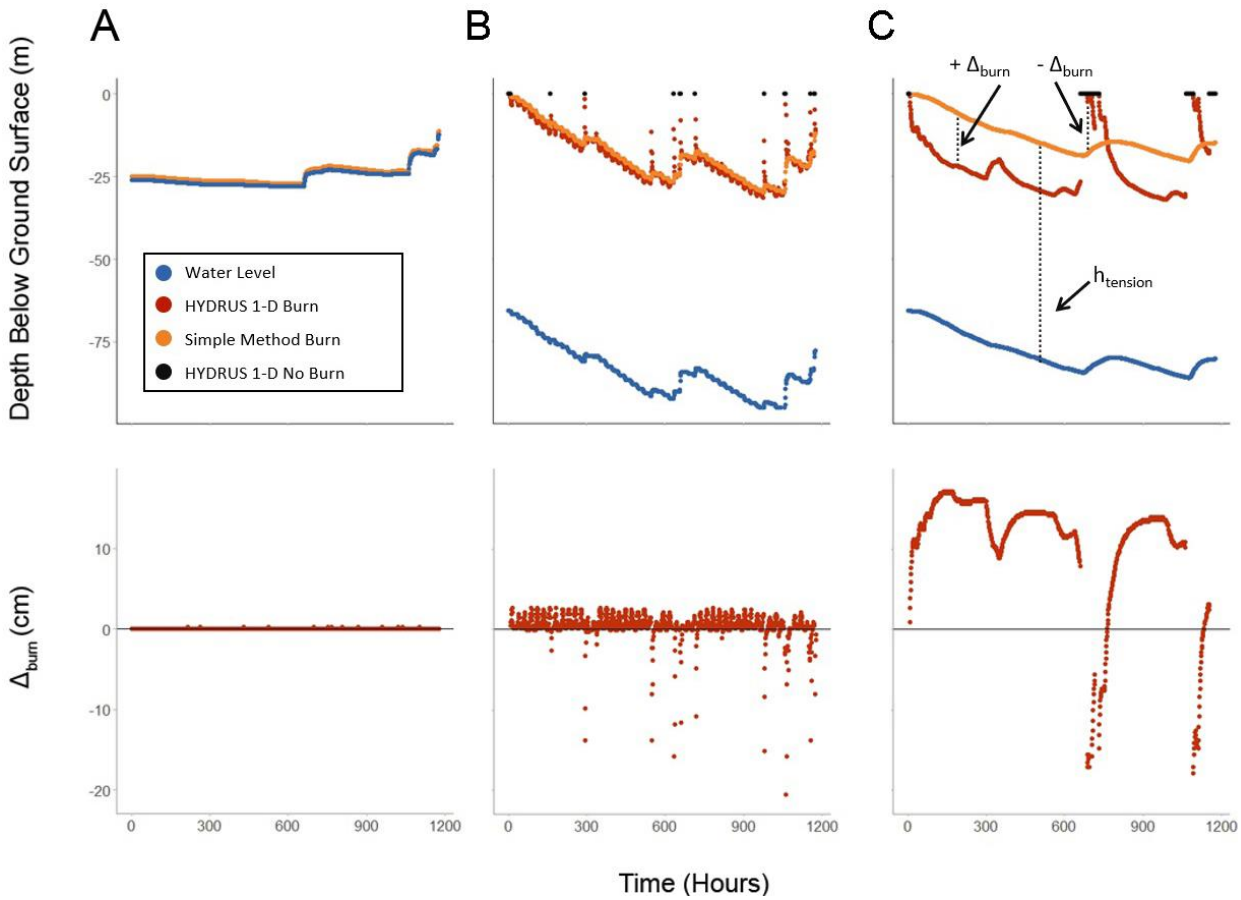

Figure 4: Modeled water tables from HYDRUS and corresponding modeled burn depths from both HYDRUS and water table-based approaches (upper panels). No burn events from the HYDRUS approach shown in black. Difference in hourly burn depth predictions between methods (Δ_{burn}) (lower panels). Site 2 Upper K_{sat} (A), Site 5 with layer appropriate K_{sat} (B) and for Site 5 with Lower K_{sat} (C).

2.3.2 Simulating Burn Depth Potentials Across Sites

Given that the comparison of modeled burn depth potentials from our subset of sites indicated that the water table-based approach is reasonable for our Upper Peats, we applied it across all 11 sites and three risk levels (L, M, H). This approach was done to compare burn depth potentials between sites and risk levels for the entire water table record (April 2017 to September 2019). Water table depths, while exhibiting similar temporal patterns, differed among sites (e.g., 3 & 9) as did their hourly burn depth potentials (shown for the H risk level in Fig. 5). Relatedly, the duration of burning risk varied among sites, with some under constant risk (e.g., Site 4) and

others never at risk (e.g., Site 5). Further, differences in $h_{tension}$ values between samples within a site created some situations where fires would burn up to a sample limit regularly (see horizontal line for Site 4 in Fig. 5), and others routinely vacillating across sample boundaries (e.g., Site 6). The mean depth of burn was also highly varied, with some sites burning incredibly shallow on average (e.g., Site 1, mean = 1.6 cm) and others deeply (e.g., Site 2, mean = 59.6 cm) (Fig. 6). Similarly, some sites exhibited a large range in burn depth potentials (e.g., Site 6, interquartile range = 44.7 cm) whereas others had a much smaller range (e.g., Site 4, interquartile range = 2.7 cm). When comparing sites for each risk level, only one pairing of sites, Sites 1 and 3 at the medium risk level, were not significantly different from one another (excluding sites that had no burning events). Notably, Sites 1 and 8 had no burning potential at the L risk level but did at the M and H risk levels (Fig. 7), highlighting the importance of $s_{smolder}$ values.

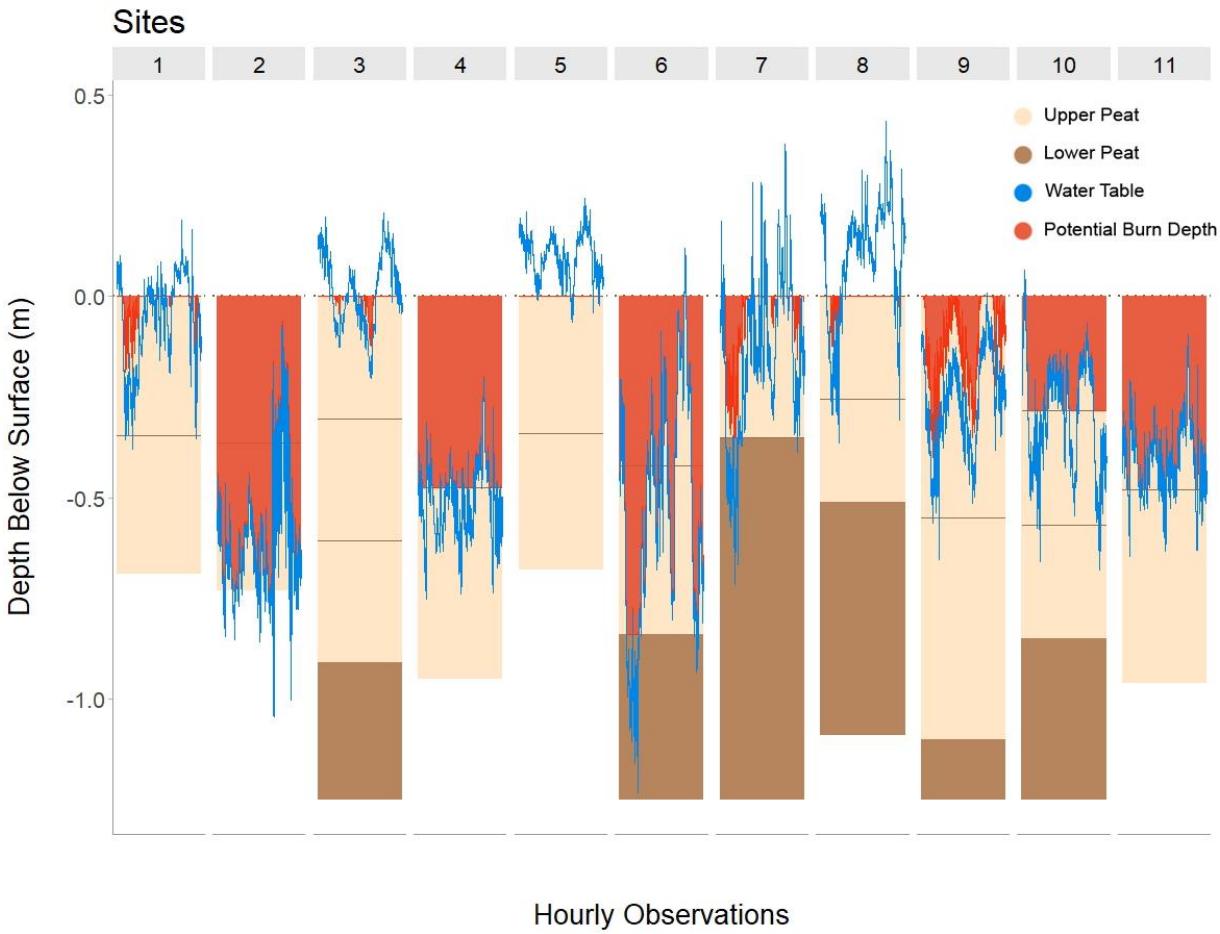

Figure 5: Burn depth potentials modeled by the water table-based method at the H risk level and observed water tables relative to ground surface across the 11 sites from April 2017 – September 2019. Total depth of Upper stratum layers shown. Lower stratum layers, where present, are truncated to 1.25 m below ground surface; Sites 1, 2 ,4, 5, & 11 had no Lower Peat present. In Site 2, the water table periodically dropped into the mineral layer. The discretization of sampled hydraulic properties is noted with horizontal lines.

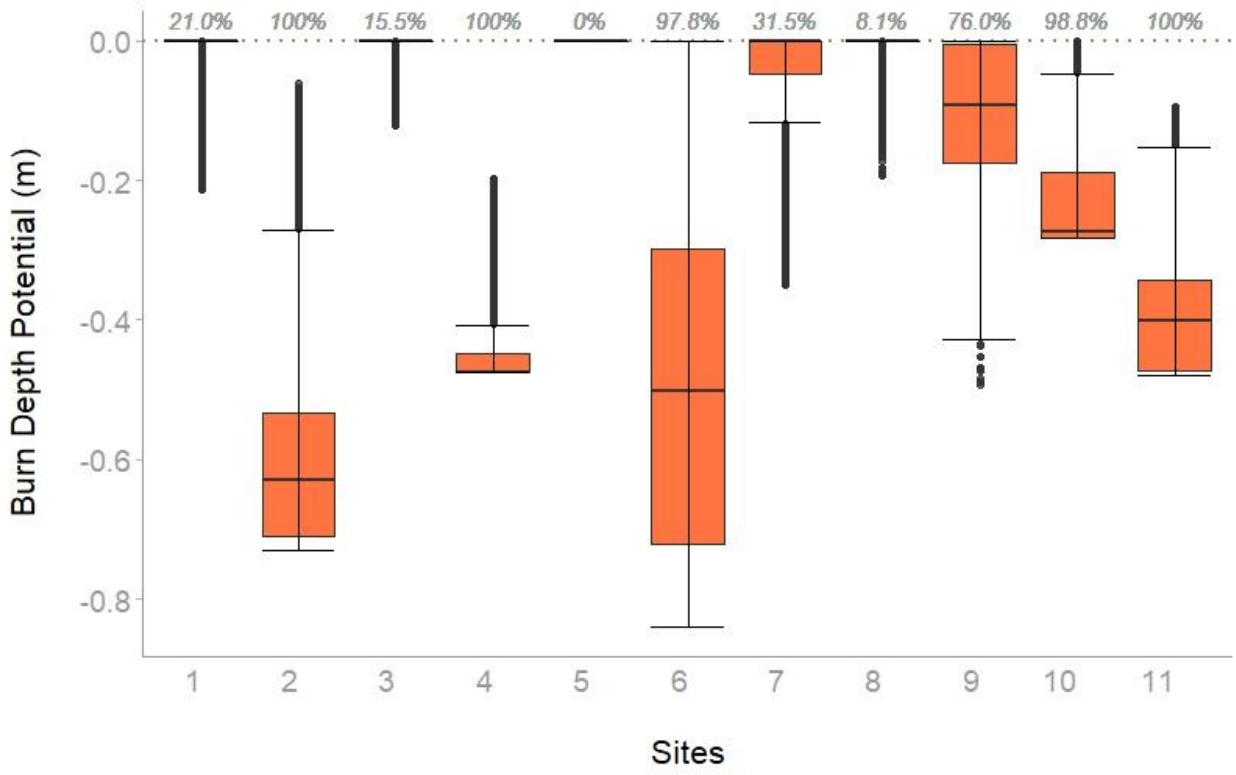

Figure 6: Burn depth potentials across the 11 sites from April 2017 – September 2019 at the H risk level, with percentage of time at risk of burning noted above each site.

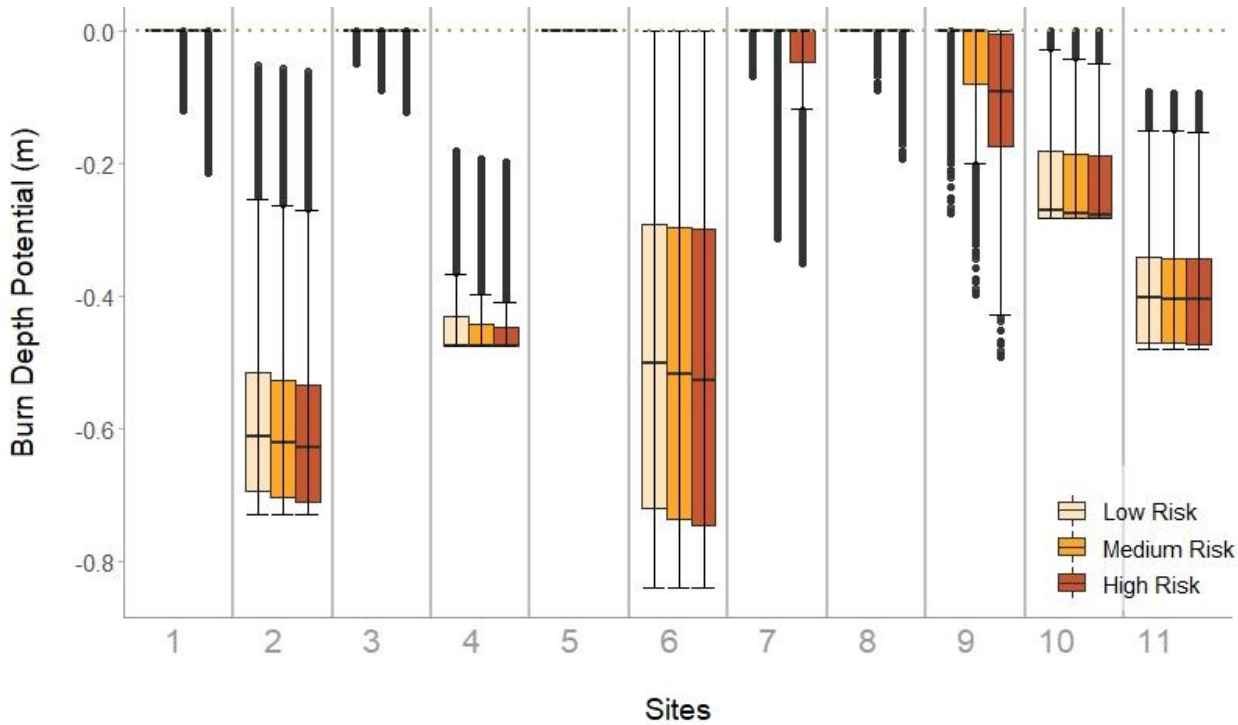

Figure 7: Burn depth potential at the three risk levels compared across the 11 sites for April 2017 – September 2019.

The relationship between mean burn depth and mean water table position was, positive and significant for all risk levels (Fig. 8A, at risk level H; $R^2 = 0.92$, p-value < 0.001). Mean burn depth also had a positive, significant relationship with the site-specific Upper-1 soil capillary length (Fig. 8B, at risk level H; Spearman's $\rho = 0.809$, p-value = 0.003). Notably, there was a significant correlation between these two controlling variables (Spearman's $\rho = 0.81$, p-value = 0.003).

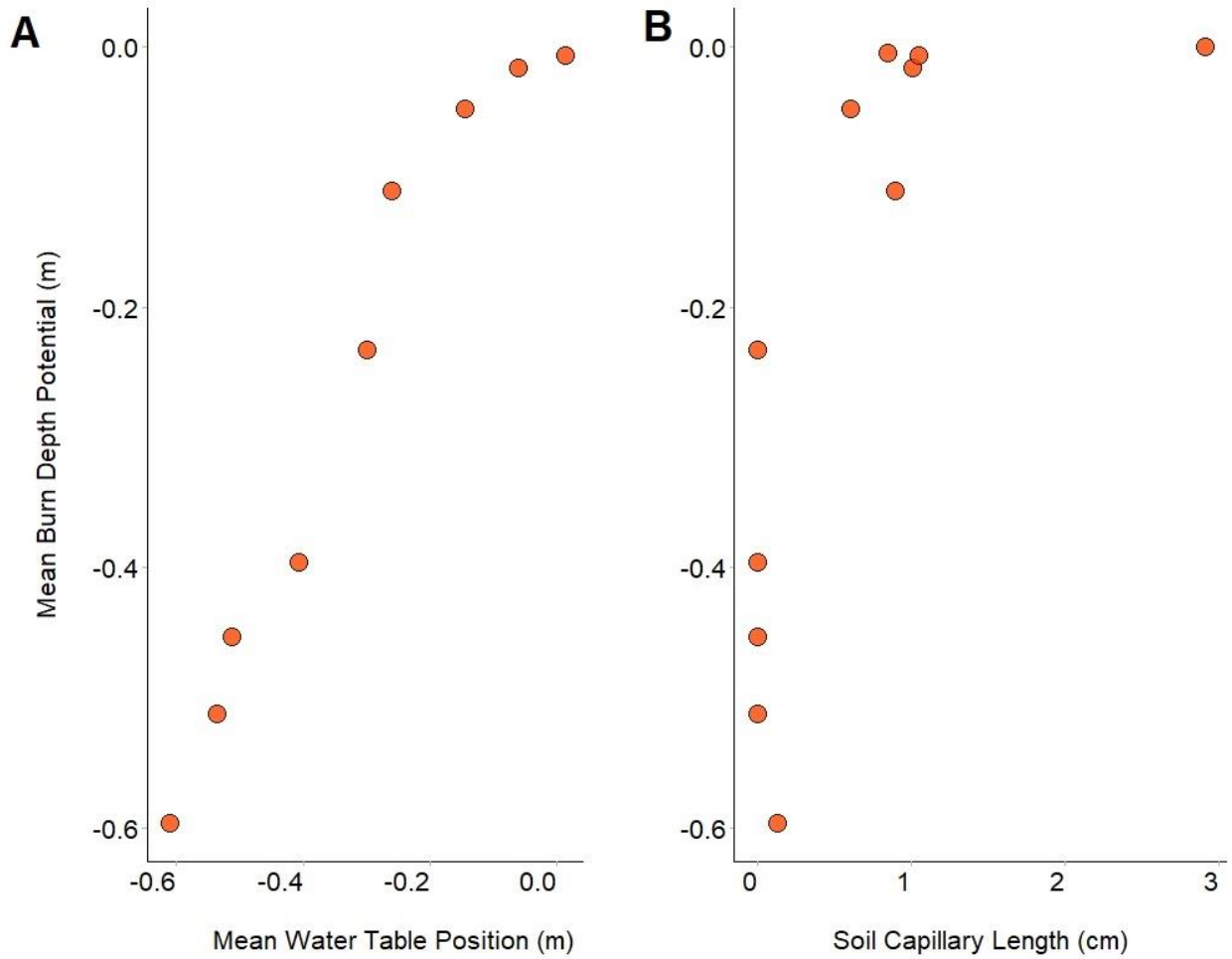

Figure 8: A) Relationship between the mean burn depth potential modeled by the water table based-approach for the highest risk level from April 2017 – September 2019 against mean water table position ($R^2 = 0.92$, p-value < 0.001) and B) against soil capillary length for the Upper-1 sample (Spearman's $\rho = 0.809$, p-value = 0.003).

2.4 DISCUSSION

In this study, we developed and verified a method of predicting burn depth potentials in organic soils. By combining depth-varying MRCs and hourly water table data with known moisture-to-ignition thresholds, we were able to model soil moisture in the vadose zone and predict depth of burn potentials across 11 sites in GDS. A subset of the results from this water table-based approach were compared against those from a more complex, process-based soil moisture model, HYDRUS- 1D. Our findings demonstrate that the former has similar

performance as the later, particularly for lower water retention soils with high K_{sat} rates. This study also highlights how inter-site variance in hydrologic regime and peat hydraulic properties can lead to differing burn depth potentials and overall fire risk within peatlands. The significant relationship between the short-term controls (water table position) and long-term controls (water retention) on burn depth potentials further emphasizes the impact drainage, and hydrologic restoration, may have on peatland fire risk and severity. Our study adds to the understanding of peat fire drivers and provides land managers and planners with a potential approach for assessing wildfire risk and prioritizing hydrologic restoration efforts.

2.4.1 Approaches to Model Burn Depth Potential

Past work in GDS peat soils focused on surface ignition predictions (Schulte et al., 2019), but here we used depth-varying MRCs to develop and test models for smoldering burn depth potentials. Peat fires can vary in severity and the amount of soil they consume, with clear implications for the global carbon balance (Kuhry, 1994; Parthum et al., 2017; Poulter et al., 2016; Turetsky et al., 2015) and local ecosystem structure (Watts et al., 2015). For example, a large fire at GDS (the 2011 Lateral West Fire) resulted in smoldering depths varying between 0 and 125 cm (mean = 47 cm) across a 25 km^2 area (Reddy et al., 2015) with large C losses (1.2 Tg C) (Hawbaker et al., 2016). In contrast, an Alaskan peat fire that burned an area over forty times in size (1039 km^2) but with shallower smoldering depths (range = 3 - 23 cm, mean = 6.1 cm) resulted in C emissions that were less than twice the amount from the Lateral West Fire (2.1 Tg C) (Mack et al., 2011). Noting both the burn depth ranges within sites and the differences between sites, it is clear that burn depths and C emissions can vary substantially both within and among peat fires. As such, the accuracy of burn depth predictions rests upon location-specific data, which requires intensive field and laboratory efforts to capture peat heterogeneity at depth

and across a site. Despite these difficulties, the importance of having such data and accurate and efficient soil moisture models extends beyond burn depth predictions and would be valuable for a range of objectives related to moisture dynamics in organic soils. Changes in peatland moisture regimes are known to impact decomposition rates and community composition (Leifeld et al., 2011; Paal et al., 2016), meaning that the methods assessed here could be used to inform a variety of management decisions.

Given the need for accurate yet feasible soil moisture models, we sought to compare the simpler water table-based approach to HYDRUS, a process-based model of soil water redistribution. HYDRUS requires known soil hydraulic properties, meteorological data, and a degree of calibration. While peat property data for HYDRUS has been fitted in previous studies for a variety of peat types and may be available (Kettridge et al., 2015; Mccarter & Price, 2014; Price & Whittington, 2010), we reemphasize the large variability in hydraulic properties both among and within peatlands (Table 1, Benscoter et al, 2011). HYDRUS simulations should be calibrated with measured water level or soil moisture data for accurate applications (Dettmann et al., 2014). Similarly, publicly available meteorological data may suffice, but model error may arise during spatially variable precipitation events (Fig. 3A). Adjustments to hydrologic input and output rates (e.g., ET:PET ratios and interception) may also be necessary depending on study region and vegetation cover. An additional issue to modeling soil moisture in peatlands with HYDRUS is that it has been shown to have trouble describing preferential and non-equilibrium flows during wetting periods as it does not account for very large macropores (Dettmann et al., 2014). Nonetheless, HYDRUS has been shown to provide a good model of soil moisture in peats (Price & Whittington, 2010), which made it useful for comparison in our study. In situations

where water table data are not available but meteorological data are, HYDRUS may be the best method to model moisture regimes in organic soils.

Compared to HYDRUS, coupling known MRCs to water table data offers a simpler approach and one easier to implement across sites and time. Employing this method still requires known hydraulic properties as HYDRUS does, but then solely relies on water table dynamics without the need for meteorological data, calibration, and more complex modeling software and skill. However, the water table-based method is only appropriate where hydrostatic equilibrium occurs rather rapidly, as was the case with our Upper Peats. In situations where rapid hydrostatic equilibration is likely not occurring (i.e., in peats that have high water retention and low K_{sat} rates), HYDRUS, or other process-based models may still be needed, depending on modeling objectives (e.g., accuracy needs, temporal resolution). Our comparison of methods suggests this may be the case for some of our Lower Peats (Fig. 4C) and the MDWP (Table 1). The water table-based approach may be valuable to assess soil moisture in drained peatlands for a variety of reasons as noted above, and future work should investigate the limits of the assumption of hydrostatic equilibrium across a variety of other organic soils.

Last, we acknowledge the uncertainty in several key parameters, namely K_{sat} and $s_{smolder}$ values. We had to rely on previous K_{sat} estimates for the HYDRUS simulations, which were different for our Upper (1678.9 cm/h) and Lower (30.48 cm/h) Peats. When adjusting K_{sat}, however, it is apparent that the extent of its influence is inherently linked to water retention. That is, sites with lower retention (e.g., Site 2) are substantially less impacted by adjustments to K_{sat} than high water retention peats (e.g., Site 5, MDWP) (Table 1). Other studies using HYDRUS to model peat moisture have similarly found that K_{sat} is a key control in high water retention peats (Kettridge et al., 2015). Our results also demonstrate that the three risk levels assessed (via three

different $s_{smolder}$ values) had subtle influences on burn depth potential, serving to adjust severity by only centimeters in either direction (Fig. 7). However, there can be substantial variation in $s_{smolder}$ values among peat types (Frandsen, 1997) and lack of precision therein, as evidenced by the large uncertainty around values applied here from Schulte et al. (2019) (e.g., H risk level $s_{smolder}$ was 71.2% with a standard deviation of 77.0%). Additional uncertainty exists around this term as the moisture content required for extinction can be much higher than the limit for ignition (Huang & Rein, 2015). Regardless of modeling approach used, the soil moisture threshold is a necessary parameter for any smoldering predictions, so we stress the importance of having a site-specific value that is as precise and accurate as possible.

2.4.2 Predictions of Burn Depth Potentials Across Sites

By applying the water table-based approach to all 11 sites, we were able to model burn depth potentials for multiple locations over a large area (Fig. 1) for a 2.5-year period of water table data (April 2017 – September 2019). Across our sites, both the site means and variances of the burn depth potentials differed (Fig. 6). During the observation window, some sites were under a constant burn threat (e.g., Site 4) whereas others never were (e.g., Site 5). The variation exhibited by our 11 sites serves to reemphasize that risk assessments should be local rather than system-wide, with implications for a range of management efforts in GDS and other peatland systems. The standard procedure to assess peat fire risk in the field is to use point-specific soil moisture data gathered by handheld sensors (Prior et al., 2020; Robichaud et al., 2004), which is applicable only for the time of measurement and not linked to potentially site-varying moisture-to-ignition thresholds. A stronger understanding of soil moisture dynamics and their specific ignition thresholds would help land managers plan prescribed burns or adjust wildfire suppression priorities around easily accessible data (e.g., water table depth), which has been of

interest in wetlands similar to GDS (Fire Environment Working Group, 2009). Further, knowledge on how the degree of risk varies spatially would help land managers prioritize sites for hydrologic restoration. Thus, future work, spanning a multitude of different peatland types, should compare modeled burn depth predictions with laboratory or *in situ* burns to further evaluate the utility of models.

The second goal of this objective was to explain the drivers of burn depth potential. The variation in water table depths across sites (Fig. 5) ultimately drove their variable burn depth predictions, clearly implicating contemporary water level regimes as the primary control of smoldering fire risk ($R^2 = 0.91$ Fig. 8A). However, the impact of site-varying peat hydraulic properties, specifically water retention, is also significant ($\rho = 0.81$, Fig. 8B), as not all sites that experienced large drawdown events were subject to deep burning (Fig. 5, e.g., Site 8 vs. Site 2). Acknowledging the strong influence that individual peat properties play on burn depth potentials, both among sites and at multiple depths within sites, further underscores the importance of site-specific soil data for accurate burn depth and fire risk predictions.

The collinearity between the two main controls on peat fire risk, water retention properties and mean water table position, demonstrates the multifaceted consequence of drainage. In the short term, a deeper water table means drier, and therefore more flammable peat. In the long term, drainage can alter peat pore structure and associated water retention properties (Peng & Horn, 2007; Peng et al., 2007; Schwärzel et al., 2002). At GDS, previous work suggested that drainage resulted in lower water retention and higher macroporosity in Upper Peat layers (Word et al., 2022). Consequently, we found that some of our sites had such poor water retention capacities that the $h_{tension}$ values in their Upper-1 samples were < 1cm (Fig. 2B). A logical extension of the combined impact of these drainage effects would be that fires in

degraded peats at GDS can regularly be expected to burn down to the water table, as was historically the assumption made by land managers at similar peatlands but refuted by other studies (Reardon et al., 2007). That extension (that drained peats may always be under threat of burning to the water table) may be a convenient shorthand assessment for risk at GDS, and is bolstered by the findings that $s_{smolder}$ values for extinction are often greater than that for ignition (Huang & Rein, 2015). However, that conclusion may not be universal as studies in drained northern bogs and fens have observed lower macroporosities (and therefore higher water retention) as compared to undisturbed peats (Kennedy & Price, 2005; Price & Schlotzhauer, 1999). These contrasting results once again emphasize the importance of site-specific assessments, particularly where past land-use has altered peats.

Considering the observed relationship between water table position and water retention properties in the reverse, our results suggest that restored peats at GDS may have fire risks more similar to undisturbed conditions. If true, this means that hydrologic restoration efforts at GDS, and potentially other peatland systems, could be an effective strategy to decrease fire vulnerability by enhancing both the short-term controls (available soil moisture) and long-term controls (water retention properties). As an example, Site 5 underwent hydrologic restoration (Balentine, 2020), has a soil capillary length within the range of the Lower Peats (Fig. 2A), and was never under risk of burning in our observation window (Fig. 6). Moreover, work comparing the properties of Upper and Lower Peats in GDS found that Upper Peats that experienced consistent saturation had hydraulic properties more comparable to undisturbed Lower Peats (Word et al., 2022). As further evidence, given that there is a relationship between pore size distribution and K_{sat} (Bouma & Anderson, 1973), K_{sat} for a peat like Site 5 may more closely align with the Lower Peat value used here (30.48 cm/h), further reducing fire risk (Table 1).

Given this, we echo the call from Rochefort & Andersen (2017) that future studies should focus on the response of peat soils to rewetting efforts. Those investigations should pay particular attention to the multiple properties (i.e., water retention, soil moisture-ignition thresholds) that drive peat flammability and if their responses to rewetting are consistent across different peatland types. Such coupled restoration and research efforts are vital to peatland revitalization (Rochefort & Andersen, 2017) and would have numerous positive benefits beyond reducing fire risk (Zedler & Kercher, 2005).

2.5 LITERATURE CITED

Allen, R. G., Pereira, L. S., Raes, D., & Smith, M. (1998). Crop Evapotranspiration—Guidelines for Computing Crop Water Requirements. Rome: Food and Agriculture Organization of the United Nations.

Balentine, K. (2020). Great Dismal Swamp NWR Design-Build Water Control Structures at GDSNWR. USFWS Report. https://doi.org/10.1017/CBO9781107415324.004

Barclay Shoemaker, W., & Sumner, D. M. (2006). Alternate corrections for estimating actual wetland evapotranspiration from potential evapotranspiration. Wetlands 26: 528–543. https://doi.org/10.1672/0277-5212(2006)26[528:ACFEAW]2.0.CO;2

Benscoter, B. W., Thompson, D. K., Waddington, J. M., Flannigan, M. D., Wotton, B. M., De Groot, W. J., & Turetsky, M. R. (2011). Interactive effects of vegetation, soil moisture and bulk density on depth of burning of thick organic soils. International Journal of Wildland Fire 20: 418–429. https://doi.org/10.1071/WF08183

Bouma, J., & Anderson, J. L. (1973). Relationships between soil structure characteristics and hydraulic conductivity. Field Soil Water Regime (pp. 77–105). wiley. https://doi.org/10.2136/sssaspecpub5.c5

Brooks, R., & Corey, A. (1964). Hydraulic properties of porous media. Hydrology Papers, Colorado State University. 1-27 Retrieved from http://www.citeulike.org/group/1336/article/711012

Bryant, M. L., Bhat, S., & Jacobs, J. M. (2005). Measurements and modeling of throughfall variability for five forest communities in the southeastern US. Journal of Hydrology 312: 95–108. https://doi.org/10.1016/j.jhydrol.2005.02.012

Dettmann, U., Bechtold, M., Frahm, E., & Tiemeyer, B. (2014). On the applicability of unimodal and bimodal van Genuchten-Mualem based models to peat and other organic soils under evaporation conditions. Journal of Hydrology 515: 103–115. https://doi.org/10.1016/j.jhydrol.2014.04.047

Dingman, S. L. (2015). Physical Hydrology: Third Edition. Retrieved from

https://books.google.com/books?hl=en&lr=&id=rUUaBgAAQBAJ&oi=fnd&pg=PR1&ots=7nJPpg9k8M&sig=qhOUrs7gz8ZwDWf7C1JjaZyqhc4#v=onepage&q&f=false

Drexler, Judith Z, Fuller, C. C., Orlando, J., Salas, A., Wurster, F. C., & Duberstein, J. A. (2017). Estimation and uncertainty of recent carbon accumulation and vertical accretion in drained and undrained forested peatlands of the southeastern USA. Journal of Geophysical Research: Biogeosciences 122: 2563–2579. https://doi.org/10.1002/2017JG003950

Drexler, Judy Z, Snyder, R. L., Spano, D., & Paw U, K. T. (2004). A review of models and micrometeorological methods used to estimate wetland evapotranspiration. Hydrological Processes 18: 2071–2101. https://doi.org/10.1002/hyp.1462

Eggleston, J. R., Decker, J. D., Finkelstein, J. S., Wurster, F. C., Misut, P. E., Sturtevant, L. P., & Speiran, G. K. (2018). Hydrologic conditions and simulation of groundwater and surface water in the Great Dismal Swamp of Virginia and North Carolina. Scientific Investigations Report. https://doi.org/10.3133/sir20185056

Fire Environment Working Group. (2009). Estimated smoldering potential. NC Fire Effects Technical Note 1.

Frandsen, W. H. (1997). Ignition probability of organic soils. Canadian Journal of Forest Research 27: 1471-1477. https://doi.org/10.1139/x97-106

Freeman, C., Ostle, N., & Kang, H. (2001). An enzymic "latch" on a global carbon store: A shortage of oxygen locks up carbon in peatlands by restraining a single enzymes. Nature 409: 149. https://doi.org/10.1038/35051650

German, E. R. (2000). Regional evaluation of evapotranspiration in the everglades. Water-Resources Investigations Report. Retrieved from http://fl.water.usgs.gov

Hansen, B. (2010). Bogged down: The dismal swamp canal. Civil Engineering Magazine Archive 80: 46–49. https://doi.org/10.1061/CIEGAG.0000538

Hawbaker, T. J., Reddy, A. D., Zhu, Z., Wurster, F. C., & Duberstein, J. A. (2016). Quantifying above and belowground carbon loss following wildfire in peatlands using repeated lidar measurements. Proceedings of the 15th International PEAT Congress: 676–680. Retrieved from http://www.peatsociety.org/document/quantifying-above-and-belowground-carbon-loss-following-wildfire-peatlands-using-repeated

Holden, J., Chapman, P. J., & Labadz, J. C. (2004). Artificial drainage of peatlands: Hydrological and hydrochemical process and wetland restoration. Progress in Physical Geography 28: 95–123. https://doi.org/10.1191/0309133304pp403ra

Huang, X., & Rein, G. (2015). Computational study of critical moisture and depth of burn in peat fires. International Journal of Wildland Fire 24: 798–808. https://doi.org/10.1071/WF14178

Joosten, H. (2010). The global peatland carbon dioxide picture. Wetland International. Retrieved from http://linkinghub.elsevier.com/retrieve/pii/S0277379111000333

Joosten, Hans, & Clarke, D. (2002). Wise use of mires and peatlands -background and principles including a framework for decision-making. International Mire Conservation Group and International Peat Society. Retrieved from www.wetlands.org/projects/GPI/default.htm

Kennedy, G. W., & Price, J. S. (2005). A conceptual model of volume-change controls on the hydrology of cutover peats. Journal of Hydrology 302: 13–27. https://doi.org/10.1016/j.jhydrol.2004.06.024

Kettridge, N., Tilak, A. S., Devito, K. J., Petrone, R. M., Mendoza, C. A., & Waddington, J. M. (2015). Moss and peat hydraulic properties are optimized to maximize peatland water use efficiency. Ecohydrology 9: 1039–1051. https://doi.org/10.1002/eco.1708

Kuhry, P. (1994). The role of fire in the development of sphagnum-dominated peatlands in western boreal Canada. The Journal of Ecology 82: 899-910. https://doi.org/10.2307/2261453

Leifeld, J., Müller, M., & Fuhrer, J. (2011). Peatland subsidence and carbon loss from drained temperate fens. Soil Use and Management, 27: 170–176. https://doi.org/10.1111/j.1475-2743.2011.00327.x

Limpens, J., Berendse, F., Blodau, C., Canadel, J. G., Freeman, C., Holden, J., … Schaepman-Strub, G. (2008). Erratum: Peatlands and the carbon cycle: From local processes to global implications a synthesis. Biogeosciences 5: 1475-1491. https://doi.org/10.5194/bg-5-1739-2008

Loveless, C. M. (1959). A study of the vegetation in the Florida everglades. Ecology 40: 1–9. https://doi.org/10.2307/1929916

Ludwig, R. F., McLaughlin, D. L., & Wurster, F. C. (2021). Red maple dominance and community homogenization in a disturbed forested wetland. Wetlands Ecology and Management 29: 599–615. https://doi.org/10.1007/s11273-021-09808-6

Mack, M. C., Bret-Harte, M. S., Hollingsworth, T. N., Jandt, R. R., Schuur, E. A. G., Shaver, G. R., & Verbyla, D. L. (2011). Carbon loss from an unprecedented Arctic tundra wildfire. Nature 475: 489–492. https://doi.org/10.1038/nature10283

Matlaga, D. P., Quintana-Ascencio, P. F., Menges, E. S., & Pickert, R. (2010). Fire mediated edge effects in bayhead tree islands. Journal of Vegetation Science 21: 190–200. https://doi.org/10.1111/j.1654-1103.2009.01132.x

Mccarter, C. P. R., & Price, J. S. (2014). Ecohydrology of sphagnum moss hummocks: Mechanisms of capitula water supply and simulated effects of evaporation. Ecohydrology 7: 33–44. https://doi.org/10.1002/eco.1313

Monteith, J. (1965). Evaporation and environment. Symposia of the Society for Experimental Biology 19: 205–234.

Natural Resources Conservation Service. (2017). Web Soil Survey. Retrieved July 7, 2021, from https://websoilsurvey.sc.egov.usda.gov/

Paal, J., Jürjendal, I., Suija, A., & Kull, A. (2016). Impact of drainage on vegetation of transitional mires in Estonia. Mires and Peat 18: 1-19. https://doi.org/10.19189/MaP.2015.OMB.183

Page, S., & Baird, A. J. (2016). Peatlands and global change: Response and resilience. Annual Review of Environment and Resources 41: 35–57.

https://doi.org/10.1146/annurev-environ-110615-085520

Parthum, B., Pindilli, E., & Hogan, D. (2017). Benefits of the fire mitigation ecosystem service in the great dismal swamp national wildlife refuge, Virginia, USA. Journal of Environmental Management 203: 375–382. https://doi.org/10.1016/j.jenvman.2017.08.018

Peng, X., & Horn, R. (2007). Anisotropic shrinkage and swelling of some organic and inorganic soils. European Journal of Soil Science 58: 98–107. https://doi.org/10.1111/j.1365-2389.2006.00808.x

Peng, X., Horn, R., & Smucker, A. (2007). Pore shrinkage dependency of inorganic and organic soils on wetting and drying cycles. Soil Science Society of America Journal 71: 1095–1104. https://doi.org/10.2136/sssaj2006.0156

Pindilli, E., Sleeter, R., & Hogan, D. (2018). Estimating the societal benefits of carbon dioxide sequestration through peatland restoration. Ecological Economics 154: 145–155. https://doi.org/10.1016/j.ecolecon.2018.08.002

Poulter, B., Christensen, N. L., & Halpin, P. N. (2006). Carbon emissions from a temperate peat fire and its relevance to interannual variability of trace atmospheric greenhouse gases. Journal of Geophysical Research 111: 1-11. https://doi.org/10.1029/2005JD006455

Prat-Guitart, N., Rein, G., Hadden, R. M., Belcher, C. M., & Yearsley, J. M. (2016). Propagation probability and spread rates of self-sustained smouldering fires under controlled moisture content and bulk density conditions. International Journal of Wildland Fire 25: 456–465. https://doi.org/10.1071/WF15103

Price, J. S., & Schlotzhauer, S. M. (1999). Importance of shrinkage and compression in determining water storage changes in peat: The case of a mined peatland. Hydrological Processes 13: 2591–2601. https://doi.org/10.1002/(SICI)1099-1085(199911)13:16<2591::AID-HYP933>3.0.CO;2-E

Price, J. S., & Whittington, P. N. (2010). Water flow in sphagnum hummocks: Mesocosm measurements and modelling. Journal of Hydrology 381: 333–340. https://doi.org/10.1016/j.jhydrol.2009.12.006

Prior, L. D., French, B. J., Storey, K., Williamson, G. J., & Bowman, D. M. J. S. (2020). Soil moisture thresholds for combustion of organic soils in western Tasmania. International Journal of Wildland Fire 29: 637-647. https://doi.org/10.1071/WF19196

R Core Team. (2020). R: a Language and Environment for Statistical Computing. R Foundation for Statistical Computing. Vienna, Austria.

Reardon, J., Hungerford, R., & Ryan, K. (2007). Factors affecting sustained smouldering in organic soils from pocosin and pond pine woodland wetlands. International Journal of Wildland Fire 16: 107–118. https://doi.org/10.1071/WF06005

Reddy, A. D., Hawbaker, T. J., Wurster, F., Zhu, Z., Ward, S., Newcomb, D., & Murray, R. (2015). Quantifying soil carbon loss and uncertainty from a peatland wildfire using multi-temporal LiDAR. Remote Sensing of Environment 170: 306–316. https://doi.org/10.1016/j.rse.2015.09.017

Rein, G. (2015). Chapter 1 - smoldering-peat megafires: The largest fires on earth. Coal and Peat Fires: a Global Perspective 4: 1-11. https://doi.org/10.1016/B978-0-444-59510-2.00001-X

Richards, L. A. (1931). Capillary conduction of liquids through porous mediums. Journal of Applied Physics 1: 318–333. https://doi.org/10.1063/1.1745010

Robichaud, P. R., Gasvoda, D. S., Hungerford, R. D., Bilskie, J., Ashmun, L. E., & Reardon, J. (2004). Measuring duff moisture content in the field using a portable meter sensitive to dielectric permittivity. International Journal of Wildland Fire 13: 343–353. https://doi.org/10.1071/WF03072

Rochefort, L., & Andersen, R. (2017). Global peatland restoration after 30 years: where are we in this mossy world? Restoration Ecology 25: 269–270. https://doi.org/10.1111/rec.12417

Schulte, M. L., McLaughlin, D. L., Wurster, F. C., Varner, J. M., Stewart, R. D., Aust, W. M., … Gile, B. (2019). Short- and long-term hydrologic controls on smouldering fire in wetland soils. International Journal of Wildland Fire 28: 177–186. https://doi.org/10.1071/WF18086

Schwärzel, K., Renger, M., Sauerbrey, R., & Wessolek, G. (2002). Soil physical characteristics of peat soils. Journal of Plant Nutrition and Soil Science 165: 479–486. https://doi.org/10.1002/1522-2624(200208)165:4<479::AID-JPLN479>3.0.CO;2-8

Simhayov, R. B., Weber, T. K. D., & Price, J. S. (2018). Saturated and unsaturated salt transport in peat from a constructed fen. Soil 4: 63–81. https://doi.org/10.5194/soil-4-63-2018

Šimůnek, J., Van Genuchten, M. T., & Šejna, M. (2006). The HYDRUS Software Package for Simulating the Two-and Three-Dimensional Movement of Water, Heat, and Multiple Solutes in Variably-Saturated Media Technical Manual.

Sleeter, R., Sleeter, B. M., Williams, B., Hogan, D., Hawbaker, T., & Zhu, Z. (2017). A carbon balance model for the great dismal swamp ecosystem. Carbon Balance and Management 12: 2-20 https://doi.org/10.1186/s13021-017-0070-4

Thompson, D. J., & Shay, J. M. (1989). First-year response of a Phragmites marsh community to seasonal burning. Canadian Journal of Botany 67: 1448–1455. https://doi.org/10.1139/b89-193

Turetsky, M. R., Benscoter, B., Page, S., Rein, G., Van Der Werf, G. R., & Watts, A. (2015). Global vulnerability of peatlands to fire and carbon loss. Nature Geoscience 8: 11–14. https://doi.org/10.1038/ngeo2325

USFWS. (2006). Great Dismal Swamp National Wildlife Refuge and Nansemond National Wildlife Refuge Final Comprehensive Conservation Plan July 2006. USFWS.

USGCRP, 2018: Second State of the Carbon Cycle Report (SOCCR2): A Sustained Assessment Report [Cavallaro, N., G. Shrestha, R. Birdsey, M. A. Mayes, R. G. Najjar, S. C. Reed, P. Romero-Lankao, and Z. Zhu (eds.)]. U.S. Global Change Research Program, Washington, DC, USA, 878 pp., https://doi.org/10.7930/SOCCR2.2018

Verry, E., Boelter, D., Päivänen, J., Nichols, D., Malterer, T., & Gafni, A. (2011). Physical properties of organic soils. Peatland Biogeochemistry and Watershed Hydrology at the

Marcell Experimental Forest (pp. 135–176). https://doi.org/10.1201/b10708-6

Watts, A. C., Schmidt, C. A., McLaughlin, D. L., & Kaplan, D. A. (2015). Hydrologic implications of smoldering fires in wetland landscapes. Freshwater Science 34: 1394–1405. https://doi.org/10.1086/683484

Word, C. S., McLaughlin, D. L., Strahm, B. D., Stewart, R. D., Varner, J. M., Wurster, F. C., … Link, N. T. (2022). Peatland drainage alters soil structure and water retention properties: implications for ecosystem function and management. Hydrological Processes 36: 1–12. https://doi.org/10.1002/hyp.14533

Zedler, J. B., & Kercher, S. (2005). Wetland resources: Status, trends, ecosystem services, and restorability. Annual Review of Environment and Resources 30: 39-74 https://doi.org/10.1146/annurev.energy.30.050504.144248

3.0 INFLUENCE OF FIRE AND DISTURBANCE-ALTERED HYDROLOGY ON THE ABUNDANCE OF *Phragmites australis*

3.1 INTRODUCTION

High severity wildfires are a disturbance of growing concern in peatlands from the artic to the tropics (Page & Baird, 2016; Page et al., 2009; Poulter et al., 2006; Turetsky et al., 2015; Usup et al., 2004). The effects of drainage, climate change, and increased burning in adjacent uplands will all likely increase the frequency of peatland fires in the coming decades (Flannigan et al., 2009; Poulter et al., 2006; Turetsky et al., 2015; Watts & Kobziar, 2013). While disturbances, including fires, are natural peatland community regulators (Loveless, 1959; Watts & Kobziar, 2013), higher fire frequency and severity increase their impact (Rein, 2015). For example, peat fires that smolder deeply through the soil profile alter topography and thus water level regimes, affecting ecosystem structure and function (Watts et al., 2015). The projected changes to fire regimes may weaken peatland resiliency to future perturbations and result in dramatic vegetation shifts (Kettridge et al., 2015).

Even in a pristine state, peatland ecosystems are prone to non-native plant invasions (Zedler & Kercher, 2004). Peatlands are especially vulnerable following disturbance, particularly changes in hydrologic regime (e.g., via drainage) (Kercher et al., 2004). Critically, as drained systems are more susceptible to deep peat consuming burns, there can be a synergistic effect where the combination of drainage and fire accelerates ecosystem degradation, further reducing resilience to invasions (Page et al., 2009). In addition to altering topography and hydrology, severe peat-consuming fires destroy regenerative material both above and below ground (Matlaga et al., 2010), all of which influences the species that recolonize post-fire (Gorham & Rochefort, 2003). Generally, invasive species are able to take advantage of degraded ecosystems (MacDougall & Turkington, 2005), but effective management of invasives requires species-

specific information about their interactions with disturbances and is therefore a primary research objective of land managers (Dix et al., 2010).

One invasive species that does exceedingly well in a post-disturbance environment and is of major management interest is the grass *Phragmites australis* (hereafter referred to as common reed) (Chimner, et al., 2016; Ji et al., 2009; Wilcox et al., 2003). Common reed is an aggressive, emergent wetland grass with annual, cane-like stems that can reach up to 6 m tall (Mal & Narine, 2003). Growing in low lying areas, common reed is most commonly found in intermittently or permanently flooded sites with still, shallow water (Haslam, 1972). Through a combination of competitive advantages, including rapid vegetative reproduction and growth (Marks et al., 1994) and abundant windblown seeds (Kettenring & Mock, 2012), common reed can quickly colonize wetlands with dense, near-monospecific stands at the detriment of native species (Farnsworth & Meyerson, 1999). Patches of common reed are comprised of the current year's growth and dead shoots from prior seasons, which hinder the establishment of other plants (Mal & Narine, 2003) and is poor habitat for many species of fish and wildlife (Able & Hagan, 2003; Robichaud & Rooney, 2017).

Given the aggressive nature of common reed, the impact it has on habitat quality, and how difficult it can be to eradicate (Farnsworth & Meyerson, 1999), it is important to identify the controls on its abundance, including the effects of fire whether direct or indirect (i.e., altered hydrology). Further, common reed patches represent a sizeable fine-fuel load on the landscape and exhibit quick recovery post-burn (Thompson & Shay, 1985), suggesting there may be a self-reinforcing grass-fire feedback cycle present (D'Antonio & Vitousek, 1992). Multiple observations have noted that regular burns facilitate common reed invasions and also maintain common reed stands by controlling less adapted competitors (Libby et al., 2002; Ward, 1968).

However, others have shown that prescribed fire can be an effective management tool for common reed in some ecosystems (Kimura & Tsuyuzaki, 2011; Marks et al., 1994; Páramo Pérez et al., 2018). The role of direct fire effects on common reed coverage aside, no studies to our knowledge have investigated the effect that fire-altered hydrology may have on its abundance. It is well understood that wetland community zonation is driven by hydrology (Hutchinson, 1967), and that common reed can be effectively managed by increasing water levels (Bart & Hartman, 2003; Hellings & Gallagher, 1992; Hudon et al., 2005; Rea, 1996; Rohal et al., 2019; Rolletschek et al., 1999; van der Valk, 1994; Weisner et al., 1993), but we do not know how an altered hydrologic regime, caused by drainage and subsequent deep smoldering peat fires, impacts its distribution.

The objective of this study was to investigate the controls on common reed occurrence and coverage, with special attention to disturbance-altered hydrology. Recent fires in a historically drained peatland in the eastern USA coastal plain (The Great Dismal Swamp) present an opportunity to observe vegetation recovery following high severity peat-consuming fires. Exploring the relationship between common reed coverage and post-fire water level regimes will enable the assessment of the impacts that drainage and deep-smoldering peat fires have had on system resiliency. We hypothesized that: H1) common reed will be more prevalent where shallow water is regularly above the ground surface; H2) greater coverage will be related to narrower hydrologic windows; and H3) the specific hydrologic conditions conducive to common reed occurrence and dominance will have been generated by a history of drainage and deep peat-consuming fires. Given the increased range of common reed in North American wetlands, the results of this investigation could have far-reaching implications for management and the understanding of grass-fire interactions.

3.2 METHODS

3.2.1 Study Area

The Great Dismal Swamp National Wildlife Refuge (GDS) is a 54,000 ha mosaic of wetland community types administered by the US Fish and Wildlife Service (USFWS) (Fig. 1). Located in southeastern Virginia and northeastern North Carolina, USA (36°35'49"N, 76°29'26"W), GDS has a temperate climate with hot and humid summers and mild winters. The main hydrologic input to GDS is precipitation, averaging 116.2 cm annually, and the main output is evapotranspiration, averaging 81.3 cm y^{-1} (USFWS, 2006). Owing to a history of intended land-use change, a series of drainage ditches segment GDS into hydrologically distinct management units. The altered hydrology of GDS has reduced species diversity across the swamp and facilitated *Acer rubrum* (red maple) into becoming the overwhelming overstory dominant (Ludwig et al., 2021). Our study site is a portion of an early seral marsh, whose boundaries were defined by a 2011 wildfire, the 2502 ha Lateral West Fire (Fig. 1).

Heavy machinery sparked the South One Fire on 09 June 2008, burning through 1,877 ha of forested peatland in GDS. Less than three years later, on 04 August 2011, a lightning strike in the South One burn scar ignited the Lateral West Fire, which burned 2,502 ha over 126 days. The conditions that led to the Lateral West Fire are postulated to be a combination of drainage, recent dry weather, and, importantly, the early successional, herbaceous community and fuel structure that returned after the South One Fire (NASA, 2022). The Lateral West Fire expanded the boundaries of the South One Fire scar and reburned much of the 1,877 ha, with the deepest smoldering occurring in the original burn scar (Parthum et al., 2017; Reddy et al., 2015). Both wildfires spread across drainage ditches and throughout the peat profile, with the 2011 wildfire

alone accounting for an average elevation loss of 47 cm and burning up to 125 cm in some locations (Reddy et al., 2015).

The vegetation community in the Lateral West burn scar is comprised primarily of herbaceous species such as *Typha latifolia* (broadleaf cattail) and *Scirpus cyperinus* (wool grass), vines of *Smilax spp.* (greenbriers) and *Rubus spp.* (brambles), and ferns, most commonly *Woodwardia virginica* (Virginia chain-fern). There is a lesser contribution from shrub species like *Morella cerifera* (wax myrtle) and *Clethra alnifolia* (sweet pepperbush), along with seedlings and saplings of tree species such as red maple and *Liquidambar styraciflua* (sweetgum). Additionally, sizeable patches of common reed exist throughout the burn scar. Herbicide treatments have been undertaken to remove common reed in some areas, but records of exact application boundaries are unclear (Fig. A-2). We are confident, however, that the management unit north of Interior Ditch (Fig. 9) did not receive any herbicide treatment prior to, or during, data collection. For this reason, we constrained our analysis of the controls on common reed occurrence to that management unit to remove the influence of herbicide treatment. However, we collected ground-truthing land cover class data points across the entire Lateral West burn scar in order to gather higher quality data to train machine learning algorithms (Fig. 9).

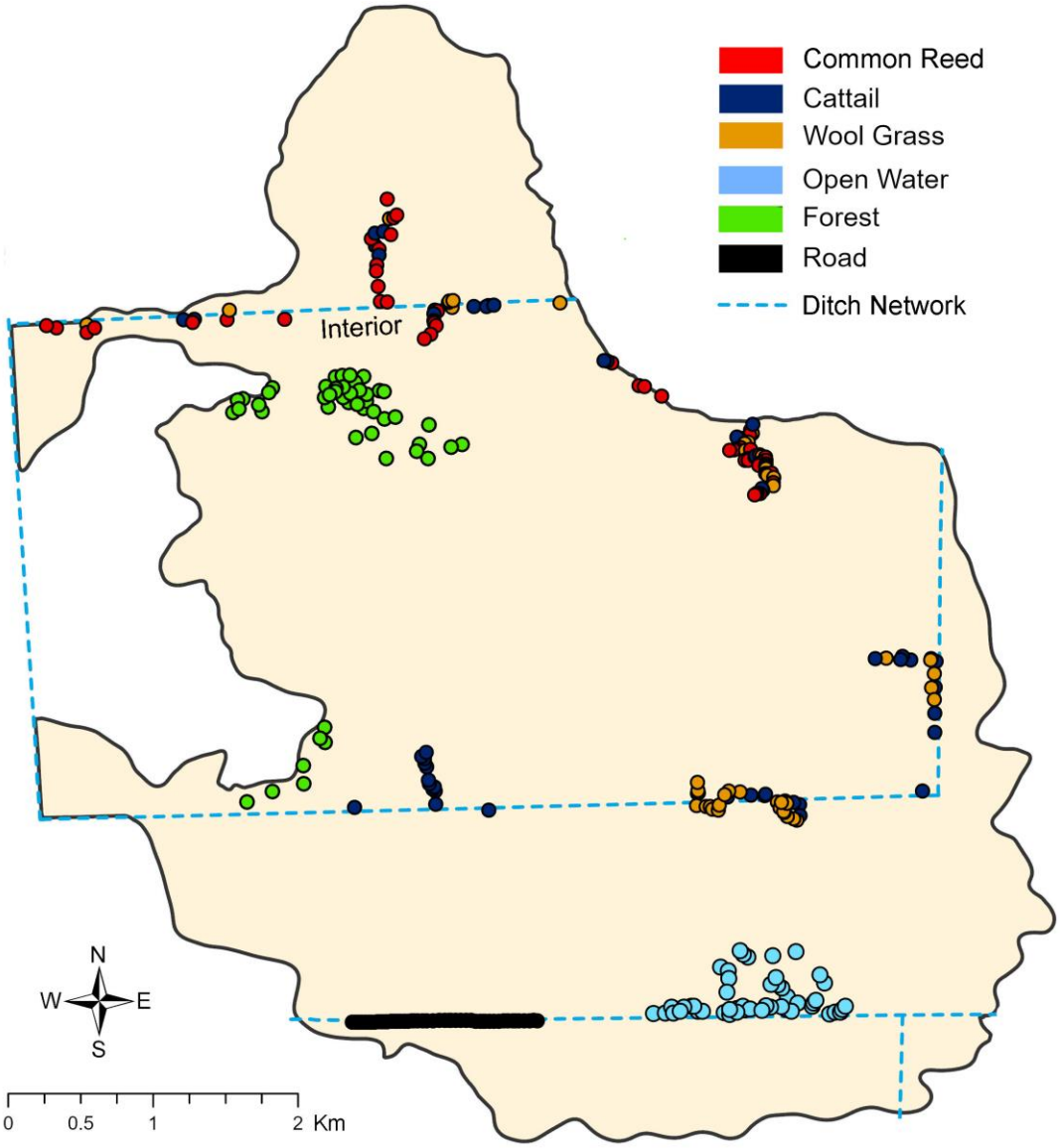

Figure 9: The Lateral West burn scar with ground-truthing data point locations and classes noted. Ditches within the burn scar are shown, and Interior Ditch is labeled.

3.2.2 Common Reed and Other Cover Class Identification

We identified multiple land cover classes, including common reed, across the study area by conducting a supervised classification of high-resolution satellite imagery. To do so, we first procured 8-band imagery of the area of interest, taken on 18 June 2021, by the WorldView-2 satellite (2.54 m resolution). This image was then preprocessed (i.e., radiometric calibration, atmospheric corrections, and scaling) by a GIS specialist from the USFWS, which enabled the

development of multiple spectral indices. The forty-four spectral indices chosen for this study (Table A-1) are ones commonly used by the USFWS (Nathan Bush, personal communication) and are the most regularly used in vegetation community delineation (L3Harris Geospatial, 2022).

To relate the values from the spectral indices to land cover classes, ground-truthing data points were collected across the Lateral West burn scar (Fig. 9). Fifty ground-truthing data points for each of three dominant cover species (common reed, cattail, and wool grass) were collected in a variety of locations and topographic settings between 15-18 June 2021. We marked the center of near monotypic patches for each class using a GPS device (Bad Elf 2200 GPS Pro, Bad Elf, West Hartford, CT, USA). An additional 50 data points for each of three broader cover types (forest, road, and open water) were manually digitized as is commonly done (e.g., Davis et al., 1995). The ground-truthing data points (n = 300) were brought into ArcGIS Pro where they were paired with the values from the forty-four spectral indices at their locations. We then split the ground-truthing data points from each of the six classes randomly into training (70%) and testing (30%) subsets so that random forest modeling, via the hold-out validation method, could be used to upscale our field observations to the remaining study area.

A nonparametric, machine learning approach, random forest modeling consists of multiple, randomly constructed decision trees that, in our application, each vote for a cover class at every pixel (Breiman, 2001). The trees are constructed utilizing a bootstrap resampling of the training subset. At each node in every tree, a random selection of spectral indices was used to find the best split (Breiman, 2001). Random forest modeling is widely used in ecology research (Cutler et al., 2007) as it is highly accurate with small sample sizes (Qi, 2012). Other studies have demonstrated that supervised classification techniques work well at identifying wetland

community types from satellite imagery, with numerous examples on common reed specifically (Lane et al., 2014; Long et al., 2017). All random forest models in this study were developed in the randomForest package in R 4.0.2 (Liaw & Wiener, 2002). Two types of output rasters were produced from the 70:30 hold-out method: a maximum likelihood raster and a probability raster. In the maximum likelihood raster, each pixel is assigned the class that received the most votes from the trees in the random forest model. In the probability raster, each pixel reports the probability of it being in each class (i.e., the number of trees that voted for each class out of the total number of trees).

We assessed the 70:30 hold-out method model by comparing the classes assigned in the maximum likelihood raster to known observations from the testing subset of ground-truthing data (following Liaw & Wiener, 2002). We generated a confusion matrix to then calculate standard classification accuracy metrics such as overall model accuracy, class-specific producer's accuracy (number of correctly classified testing data points divided by the total number of ground-truthing data points), and class-specific user's accuracy (number of correctly classified testing data points divided by the total number of points determined to be that class). These metrics were compared to the same metrics from a tenfold cross validation approach to further evaluate the accuracy of the 70:30 hold-out method. For the tenfold cross validation approach, the ground-truthing data were split into ten unique 90:10 training to testing sets (Refaeilzadeh et al., 2016). With these, ten unique random forest models were developed, and their confusion matrices were merged. This method is more conservative and utilizes all data for training across the ten models. However, the tenfold method was only used to evaluate the 70:30 hold-out method as the former does not produce a probability raster, which was needed to create the final, presence-or-absence output raster.

We transformed the probability raster into binary, presence-or-absence observations for each class as is standard for species distribution models. This transformation was done using class-specific probability thresholds defined by another accuracy metric of the 70:30 hold-out method, the True Skill Statistic (TSS). TSS is calculated by summing Sensitivity (the probability that the model will correctly predict presences for that class (0-1)) and Specificity (the probability that the model will correctly predict absences for that class (0-1)) and subtracting one (Allouche et al., 2006). For each pixel in the probability raster, any class probability greater than or equal to its TSS was deemed a present observation for that class. TSS has been shown to be a reliable probability cut-off for use in species distribution models (Allouche et al., 2006) and has been used in other studies as a threshold for presence or absence of common reed specifically (Long et al., 2017). This approach allowed us to upscale our observations in a way that was rooted in the confidence we had in the accuracy of our supervised classification.

We assessed the degree of spatial autocorrelation among common reed observations to evaluate if systematic spatial variation explained common reed distribution, if that influence was scale dependent, and thus if analysis of common reed occurrence and its controls warranted a multi-scale approach. Moran's I, a correlation coefficient specifically developed as a measure of spatial autocorrelation (Moran, 1950), was calculated at ten neighborhood sizes (2.54 m to 25.4 m in one pixel increments) to elucidate how the degree of dispersion changes as the search area increases. Moran's I is on a +1 to -1 scale, where +1 indicates perfect clustering and -1 indicates perfect dispersion. The results from the Moran's I sensitivity analysis clearly demonstrated that common reed observations exhibited a high degree of clustering at a fine resolution, but that this phenomenon was scale dependent (Fig. 10). At the one-pixel neighborhood scale (2.54 m

resolution), the Moran's I value was 0.65 as compared to the ten-pixel neighborhood scale, where I was 0.32.

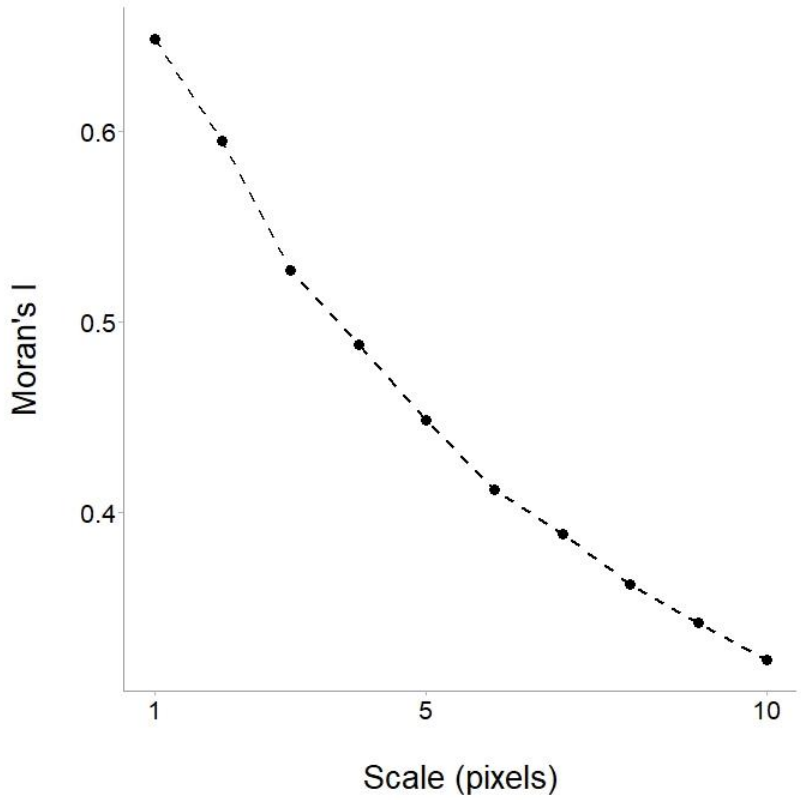

Figure 10: Moran's I sensitivity analysis, demonstrating the scale dependence of spatial autocorrelation from one- to ten-pixel neighborhood scales.

Given the scale dependency of spatial autocorrelation, we chose to assess common reed occurrence and coverage, and its potential controls, at three different spatial resolutions. The binary, presence-or-absence rasters, at the resolution of our original satellite imagery (2.54 m resolution), were the basis for our pixel-level analysis. We then up-sampled at a three-pixel resolution to generate kernels (7.62 m). The kernel values were pseudo coverages, with the summation of all positive observations (0-9) divided by the total number of observations (9). We repeated this process at a nine-pixel resolution to generate an even larger spatial resolution (22.86 m), called super kernels (0-81 out of 81) (Fig. 11).

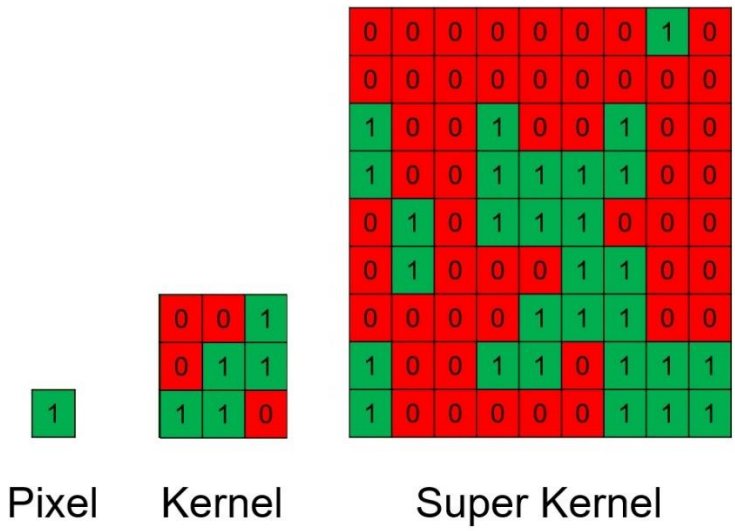

Figure 11: Schematic of a binary, pixel raster cell (2.54 m resolution), and a kernel (7.62 m resolution) and super kernel (22.86 m resolution) up-sampled from the pixel. Green and 1 denote presence, red and 0 denote absence. Kernel example is 55.5% coverage, super kernel example is 35.8% coverage.

3.2.3 Relationships Between Common Reed Coverage and Environmental Variables

To understand the controls on common reed abundance, we gathered data for multiple environmental variables across our study site (Fig. 12). Hydrology was characterized by combining a series of hourly water table observations with a digital elevation model (DEM). The DEM, provided by the USFWS, was developed from LiDAR data collected in August 2012, immediately after the Lateral West Fire was extinguished. Captured during a dry period and before much of the vegetation returned, the data are considered true to ground surface. The LiDAR data (2 m resolution) has a 7 cm root mean square vertical error compared to known control points. The water table was monitored with two wells, each fitted with submersible, vented, pressure transducers (HOBO U20L-04 data logger, Onset Computer Corporation, Bourne, MA, USA), that were installed in August 2020 and collected continuous hourly data until November 2021 (Fig. 12). We chose the well locations to confirm that the water table is flat. To do so, the hourly water table observations were converted to water table elevations (via

the DEM values at the well locations) and the relationship between synchronous well observations was assessed using a simple linear regression. Results from that analysis confirm that the water table is flat ($y = 1.02x – 0.53$ and $R^2 = 0.97$) (Fig. 13). The 2 m resolution of the DEM simplifies microtopographic heterogeneity which likely explains why the intercept shows an offset between observations. Additionally, as the slope is near 1 we are confident that the water table is flat. Thus, we generated a 2 m raster of mean water table position relative to ground surface (hereafter water level) across our study site by combining the mean water table elevation at well 1 with the DEM.

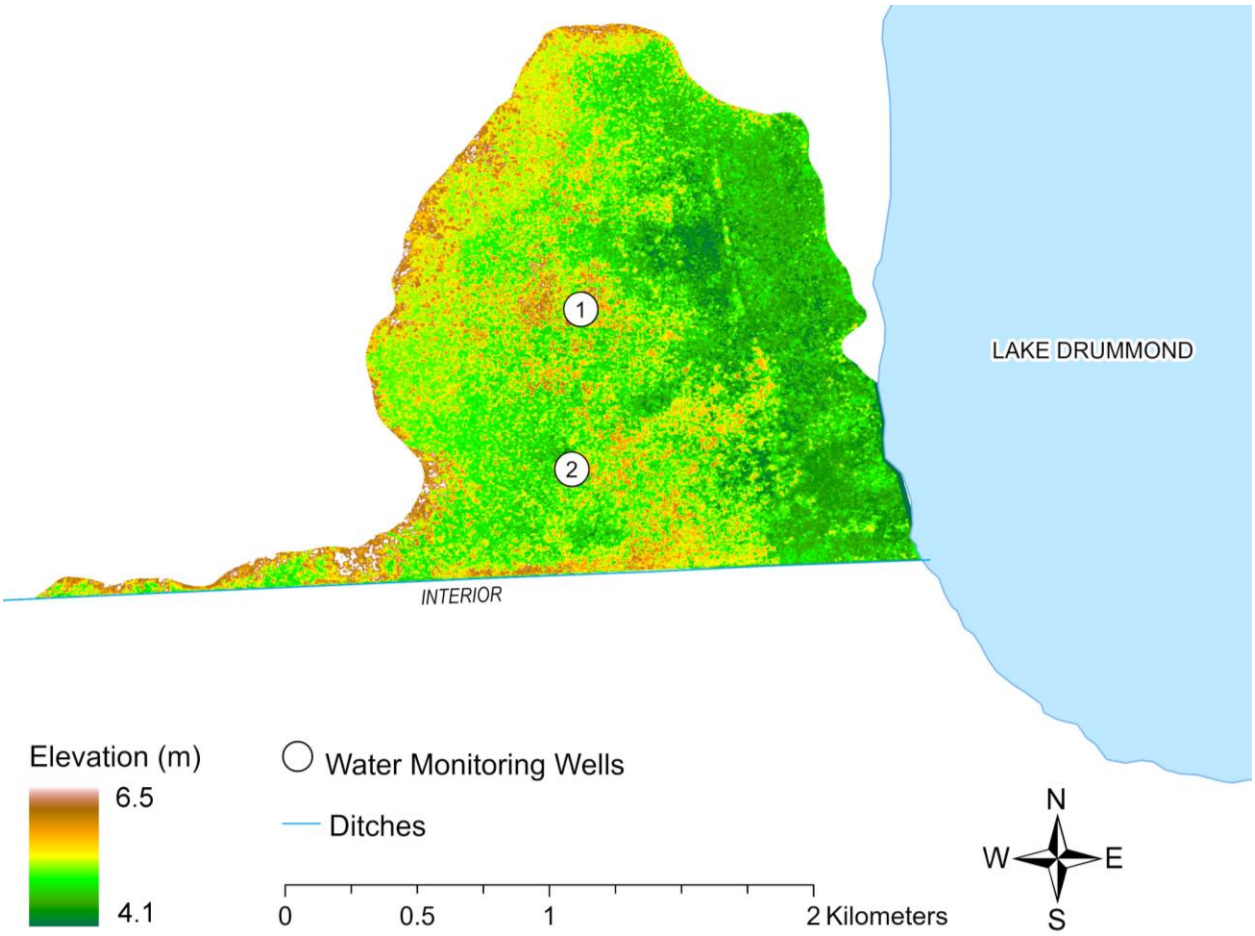

Figure 12: Study site north of Interior Ditch along with well locations and the LiDAR-derived digital elevation model.

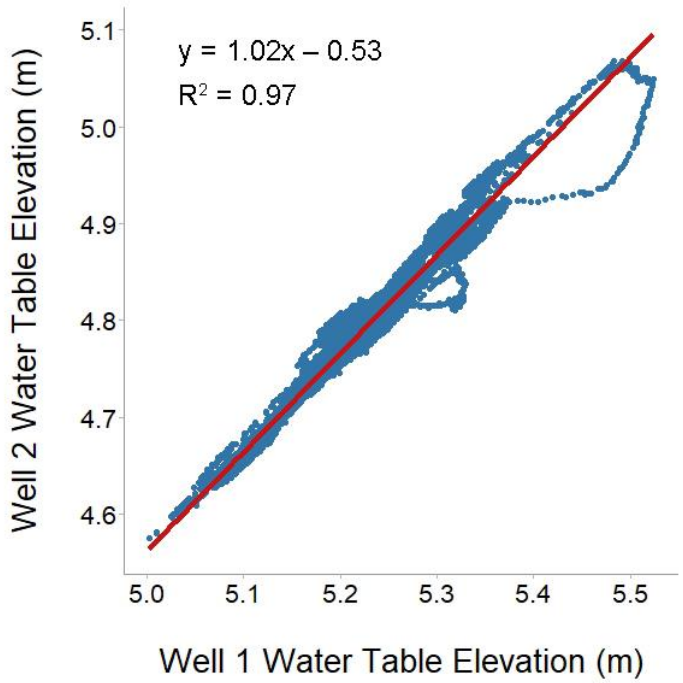

Figure 13: Linear regression between synchronous water table elevations at Wells 1 and 2.

To evaluate the influence of environmental variables on common reed occurrence at the pixel, kernel, and super kernel resolutions, rasters of the same size and resolution were developed. The water level raster (2 m resolution) was resampled via bilinear interpolation to match the resolution of the binary, presence-or-absence rasters (2.54 m resolution). The water level raster was then up-sampled to match the kernel and super kernel resolutions, and their values were the average of their pixel components. A burn raster was generated from shapefiles that delineated the boundaries of both the 2008 and 2011 burn scars. The burn boundary shapefiles were previously created from a combination of aerial surveys and satellite imagery by the USFWS staff at GDS. In areas where both shapefiles were present, the raster value noted two burns and in areas where only one was present the raster value noted a single burn. As roadways and open water are known to be vectors of transport for common reed (Maheu-Giroux & De Blois, 2007), the shortest distance to each was calculated for each pixel. Those values were up-

sampled at the two larger spatial resolutions by selecting the median pixel value for each kernel or super kernel.

The relationship between common reed distribution and hydrology was tested at the three different spatial resolutions (pixel, kernel, and super kernel). At the pixel resolution, water levels were compared between presences and absences with a Wilcoxon rank sum test ($\alpha = 0.05$ for this and all following tests). For kernels and super kernels, water levels were compared between the coverage values (i.e., 0-9 for kernels and 0-81 for super kernels) with Kruskal-Wallis H tests and post-hoc, pairwise Wilcoxon rank sum tests. In addition, we calculated the mean water level for each coverage value and assessed the relationship between water level and coverage using Spearman's correlation analyses at both the kernel and super kernel resolutions.

As an investigation of the potential impact that multiple fires have on common reed occurrence, we compared the proportion of presence to absence observations between the once and twice burned areas at the pixel resolution with a Pearson's Chi-squared test. Additionally, the water levels were compared between burn levels to investigate a potentially confounding factor (i.e., altered hydrology caused by deep, peat-consuming fires) on the relationship between times burned and common reed presence using a Wilcoxon rank sum test.

To evaluate how multiple environmental factors, along with the effects of spatial autocorrelation, influence common reed occurrence and coverage, we ran auto-logistic regressions at all three resolutions. An auto-logistic regression is a spatially lagged binomial logistic regression that includes a lagged auto-covariance term that accounts for the effects of spatial autocorrelation (Evans & Murphy, 2021). Our models included water level, distance to nearest road, and distance to nearest open water as independent factors along with the lagged auto-covariate term as a nuisance variable. To relate the relative importance of each independent

factor on common reed occurrence and coverage, we converted the regression coefficients from log-odds to odds. To assess the explanatory power of the models, we calculated pseudo coefficients of determination, Nagelkerke's R^2, for all three auto-logistic regressions. All auto-logistic regression models were constructed in the spatialEco package (Evans & Murphy, 2021). All statistical tests and comparisons were conducted in R 4.0.2 (R Core Team, 2020).

3.3 RESULTS

3.3.1 Common Reed and Other Cover Class Identification

The supervised classification via the 70:30 hold-out method had an overall accuracy of 85.2%. Class-specific accuracy terms from the 70:30 hold-out method (Table 2) further imply success with this approach, and they are greater than values reported in literature that utilized a similar method to identify wetland cover classes, including common reed (Long et al., 2017).

Table 2: Classification accuracy terms from the random forest models for both the 70:30 hold-out and the tenfold cross validation methods for each cover class. All values are percentages. Producer's accuracy is the number of correctly classified testing points divided by the total number of testing points. User's accuracy is the number of correctly classified testing points divided by the total number of points determined to be that class. TSS is the summation of the probabilities that the model correctly identifies presences and absences minus one.

Cover Class	Producer's Accuracy		User's Accuracy		True Skill Statistic (TSS)	
	70:30	Tenfold	70:30	Tenfold	70:30	Tenfold
Common Reed	82.4	90.0	87.5	88.2	80.0	88.8
Cattail	75.0	74.0	65.2	71.2	65.1	68.8
Wool Grass	64.7	76.0	68.8	80.9	58.8	71.3
Forest	100	98.0	100	94.2	100	97.6
Open Water	91.7	94.0	100	97.9	91.7	92.8
Road	100	100	100	100	100	100

The class specific accuracy metrics from the tenfold cross validation approach are higher in some cases than the same metrics from the 70:30 hold-out approach (Table 2). Notably, the classes that saw the largest differences were the species-specific classes (common reed, cattail, and wool grass). It is understandable that the tenfold cross validation approach would have stronger accuracy metrics considering the size of our ground-truthing dataset, but the close agreement between the two methods further indicates good performance by the 70:30 hold-out approach. Again, we note that probability rasters are not a possible output via the tenfold method. Given this, we used the probability raster generated from the 70:30 hold-out method to make the binary, presence-or-absence class rasters with the TSS thresholds. The final presence-or-absence map (Fig. 14) demonstrates the colony structure and shape of common reed that we expected given the biology of the species (Mal & Narine, 2003). Additionally, the locations where common reed was modeled closely align with observations made by the USFWS in an aerial survey conducted in 2020 (Fig. A-1). The other five cover classes were regularly modeled in locations as expected from cursory field observations, further bolstering confidence in our model performance.

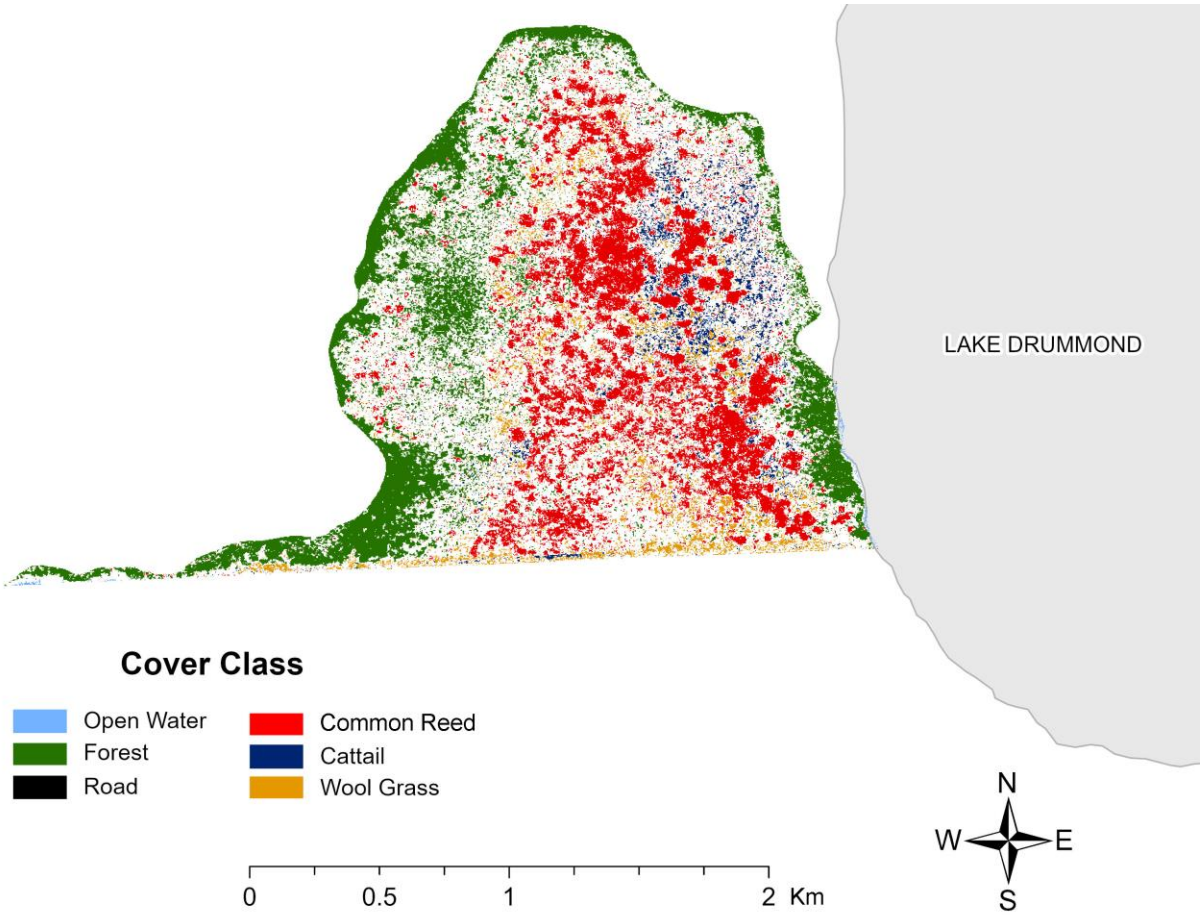

Figure 14: Map of the modeled land cover classes as produced by the supervised classification of high-resolution satellite imagery (2.54 m). White space denotes areas where no one class was confidently predicted by the models.

3.3.2 Relationship Between Common Reed Coverage and Environmental Variables

At the binary, pixel resolution, there were significant differences between water levels for presences and absences (p-value < 0.0001) (Fig. 15A). The median water level for presences was 0.18 m above ground and the median for absences was 0.09 m, which implies a smaller degree of divergence than indicated by their strong statistical difference. At the kernel level, the highest (100%) and lowest (0%) common reed coverages had water levels that were significantly different from each other and from the intermediate coverages (p-values < 0.0001), but many of the internal coverages were not significantly different from one another (Fig. 15B). At the super

kernel level, a similar general pattern held where many internal coverages did not significantly differ in their water levels from other internal coverages, and the extremes (0% and 100%) were significantly different from each other and many of the internal coverages (Fig. 15D). Notable at all resolutions, the range of water levels tended to be narrower as coverage increased (or presence as compared to absence at the pixel resolution) (Fig. 15A, B, & D).

Results from the Spearman's correlation analyses indicate strong, significant positive relationships between the coverages and their mean water levels at both the kernel and super kernel levels ($\rho = 0.95$, p-value < 0.0001 and $\rho = 0.81$, p-value < 0.0001 respectively) (Fig. 15C & E). These relationships are simplifications of the overlapping water levels demonstrated by the Kruskal-Wallis H tests but serve to better illustrate the relationship trend that exists between increasing water level and common reed coverage.

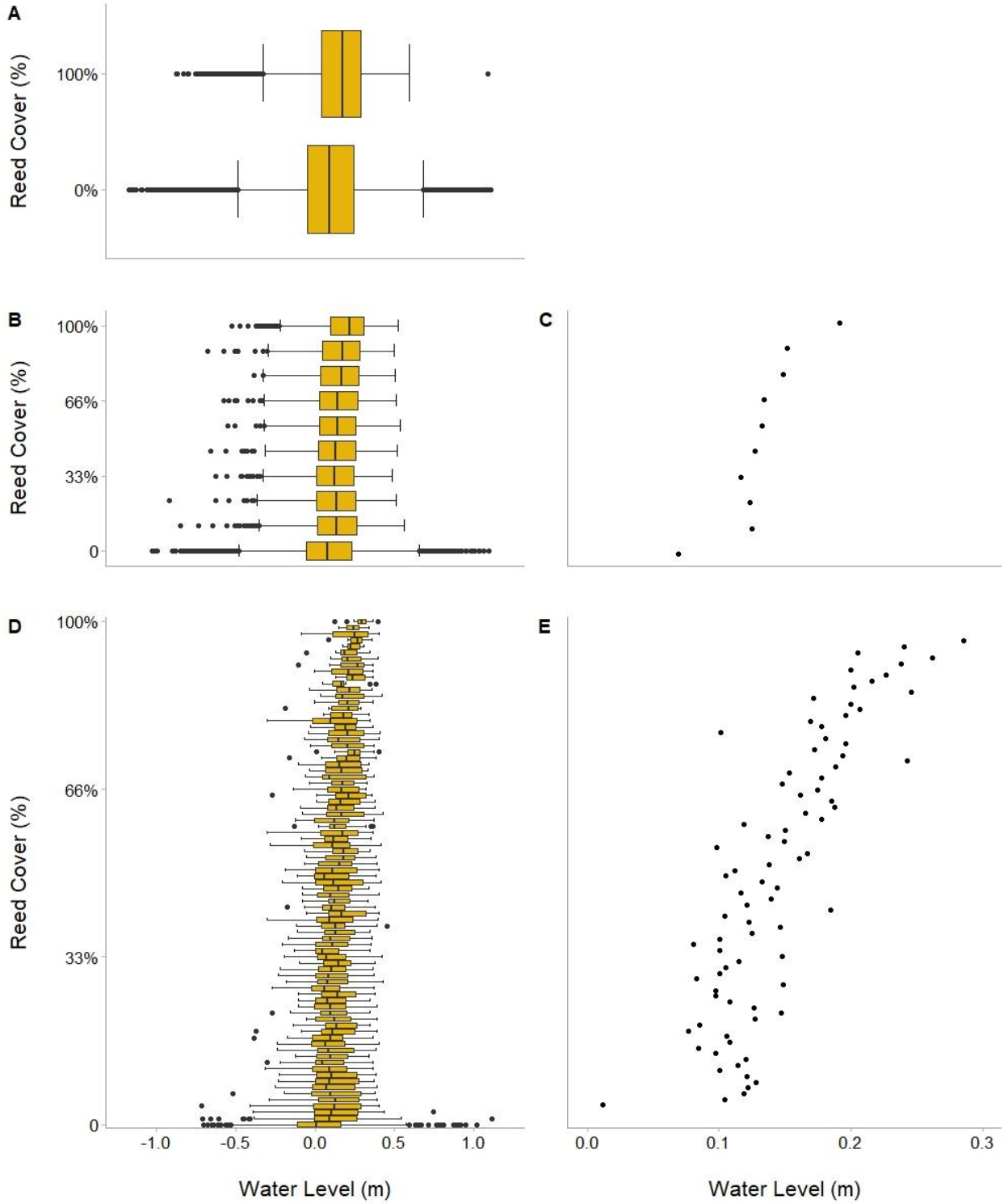

Figure 15: A) Water level distribution of presence and absence observations at the pixel resolution. B) Water level distributions for each of the kernel coverages. C) Kernel coverages vs. their mean water levels ($\rho = 0.95$). D) Water level distributions for each of the super kernel coverages. E) Super kernel coverages vs. their mean water levels ($\rho = 0.81$).

There was a significant difference between the proportion of presence to absence observations in the two burn levels (p-value < 0.0001). In the area that burned once, only 3.30% of observations had common reed present, whereas in the area that burned twice 29.92% of observations had reed present (Fig. 16).

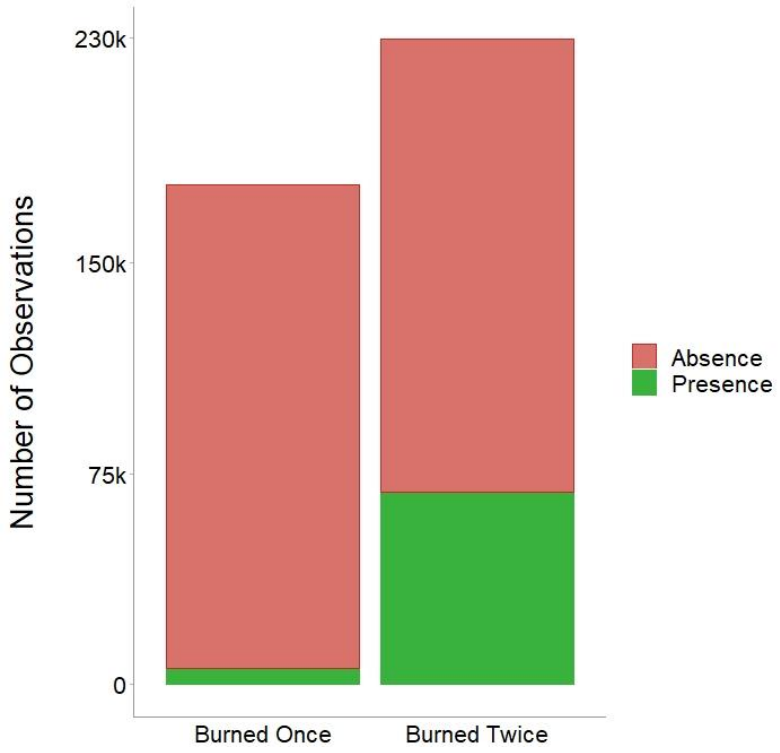

Figure 16: Number of presence and absence observations for the areas that burned once and twice. Areas that burned once had 3.30% present observations; areas that burned twice had 29.92% present observations.

Water levels in areas that had burned twice were significantly higher than the areas that burned once (p-value < 0.0001). Areas that burned once had a median water level of 0.02 m whereas the area that had burned twice had a median water level of 0.14 m. Additionally, the distribution of water levels in areas that burned twice was more left skewed, indicating further separation in the hydrology of the two burn levels (Fig. 17).

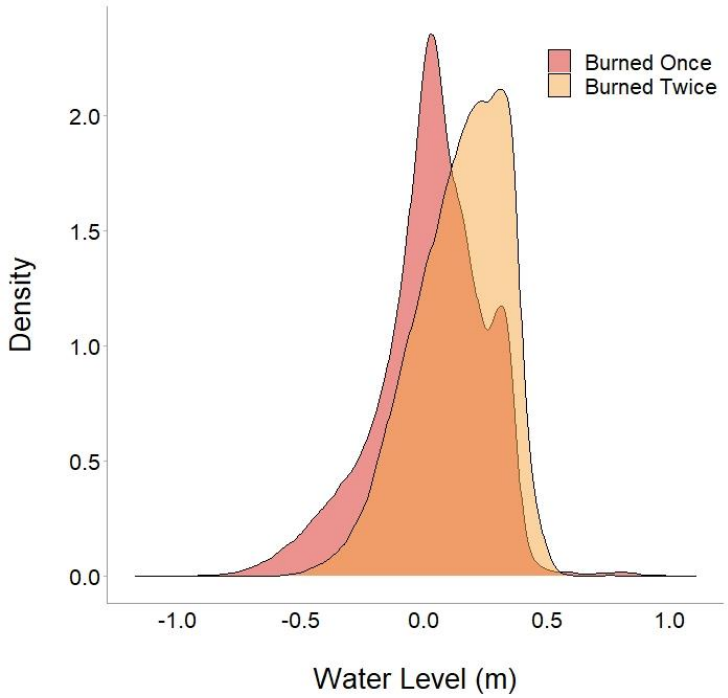

Figure 17: Density plots of water levels for both burn levels. Notably, the areas that have burned twice are wetter on average (0.02 m compared to 0.14 m) and are more left skewed.

Results from the auto-logistic regression at the pixel resolution highlighted the importance of spatial autocorrelation on common reed presence at that scale (Table 3). As the resolution increased, the impact that spatial autocorrelation had on common reed coverage decreased and was supplanted by the increasing importance in water level. These results align with our findings from the Moran's I sensitivity analysis. All models demonstrate that the distances to nearest road and nearest open water were non-important.

Table 3: Regression coefficients from the three auto-logistic regression models reported as odds. Nagelkerke's R^2 values reported.

Resolution	Water Level	Distance to Nearest Road	Distance to Nearest Open Water	Spatial Autocorrelation	R^2
Pixel	1.59	1.00	1.00	1102.16	0.71
Kernel	1.77	1.00	1.00	1.11	0.66
Super Kernel	2.65	1.00	1.00	1.16	0.65

3.4 DISCUSSION

In this study we sought to understand the patterns and controls of common reed occurrence in a large peat fire scar at GDS, with special attention towards the unique, disturbance-generated hydrologic conditions present. To do so, we identified common reed occurrence via a supervised classification of high-resolution satellite imagery and gathered data on a series of site-specific factors. By pairing the common reed observations with water level data, we observed increased common reed abundance in areas with generally higher water levels at multiple spatial resolutions. We also found paired phenomena: areas that had burned twice had more common reed and were wetter on average. While the effect of spatial autocorrelation played a large role on common reed occurrence, its relative influence was diminished at larger spatial resolutions where the role of hydrology was again a key explanatory variable. The findings from this study add to our understanding of the influence that fire and disturbance-altered hydrology have on common reed invasions and may aid land managers in removal efforts.

3.4.1 Influence of Hydrology on Common Reed

The influence of water level regimes on common reed occurrence at GDS was evident at all spatial resolutions. At the binary, pixel resolution, common reed observations occurred in significantly wetter locations on average and occupied a smaller hydrologic window than locations where it was absent (Fig. 15A). At both the kernel and super kernel resolutions, greater reed coverages were related to higher water levels (Fig. 15C & E), demonstrating that higher density common reed patches, which are likely patch or colony centers, are in wetter locations. These patch centers also have small ranges of variability in their water levels (Fig. 15B & D), which further implies that these locations are ideal hydrologic settings for common reed.

Numerous other studies have shown that flooding can control common reed (Bart & Hartman, 2003; Hellings & Gallagher, 1992; Hudon et al., 2005; Rea, 1996; Rohal et al., 2019; Rolletschek et al., 1999; van der Valk, 1994; Weisner et al., 1993), which seemingly contrasts our findings of higher density common reed in wetter areas. However, the 'wetter' sites in our study are only wetter in a relative sense as the 100% coverage sites in the super kernel analysis had a mean water level of only 0.29 m. Hudon et al. (2005) found that a site needed to be regularly inundated with water levels up to 0.5 m to be inhospitable to common reed, and Weisner et al. (1993) found that water levels at or above 0.8 m significantly limited common reed growth. Additionally, the range of our absence observations extended into wetter sites than the presence observations, suggesting that there are locations too wet for common reed to establish or succeed in our study site.

Our findings imply that high density common reed patches are found where the hydrologic setting is ideal. The smaller coverages in our study site exhibited a wider range of water level conditions and likely represent patch edges, small patches, or first year growth far from the colony interior. Vigorous colonies have the capacity to expand into less suitable habitat space through vegetative reproduction and clonal expansion (Amsberry et al., 2000), potentially explaining the wider hydrologic conditions observed for lower coverages. While traditional horizontal growth is only around 1 m annually, long stolons called legehalme can extend up to 15 m horizontally, greatly expanding the reach of a colony and allowing it to test the viability of locations far from the patch interior (Mal & Narine, 2003). Both living and dead shoots act as aerenchyma tissue that can transport oxygen to shoots experiencing anoxic stress in wetter locations, thereby supporting colony growth into less preferred conditions (Mal & Narine, 2003).

The importance of vegetative expansion and the colony structure of common reed was also supported by the Moran's I sensitivity and regression analyses, both of which demonstrated the scale dependency of spatial autocorrelation (Fig. 10, Table 3). This result is unsurprising given the fine resolution of the pixel scale (2.54 m), which is likely smaller than many reed patches. It then follows that being near other common reed observations would be a strong predictor variable. Additionally, vegetative reproduction allows common reed colonies to expand outward seasonally at a steady rate, and likely into more unsuitable hydrologic conditions, further explaining why we found a high degree of spatial autocorrelation, and smaller influence of hydrology, at our smallest resolution. At larger resolutions (7.62 m and 22.86 m), high reed coverages may have been representing patches in their entirety, therefore reducing the importance of spatial relationships. However, proximity to a viable seed source is still an important factor in determining common reed occurrence and may explain why we observed odds greater than 1 for spatial autocorrelation at the larger resolutions. Those regression coefficients were lower – and coefficients for water level influences higher – at the kernel and super kernel resolutions likely because hydrology plays a larger role in the success of sexual reproduction compared to vegetative expansion, as reed seeds struggle to germinate outside of preferred hydrologic conditions (Hudon et al., 2005). The contributions of distance to nearest ditch and open water were less significant in explaining common reed occurrence, as propagule dissemination, while a viable reproductive pathway, is less common than clonal expansion (Amsberry et al., 2000). Given this, the degree of spatial autocorrelation was more important in explaining where common reed was found compared to the closest distance to invasion vectors, which aligns with findings in other ditched wetlands (Maheu-Giroux & De Blois, 2007).

3.4.2 Phragmites-Fire Feedbacks

Our findings support the notion that there may be positive feedbacks between common reed and fire in disturbed peatlands. The comparison of proportions of common reed presences-to-absences in the once and twice burned areas demonstrates that there was significantly more common reed in the areas that burned multiple times (3.30% positive to 29.92% positive respectively) (Fig. 16). Additionally, the comparison of water levels shows that the twice burned areas were wetter on average (Fig. 17). These two results indicate that high severity, peat-consuming fires may have indirect, positive effects on common reed invasion through alterations to topography and thus hydrology and give credence to the idea that high-severity fires in peatlands help fuel common reed invasions.

As further support for this hypothesis, regular fires remove vegetation and support fire tolerant species (Loveless, 1959; Ward, 1968), including common reed, which in a post-burn environment can rapidly establish dense, monospecific stands (Ji et al., 2009; Wilcox et al., 2003). It has been demonstrated experimentally that burning common reed promotes bud development and increases stem density (Cowie et al., 1992; Ostendorp, 1999), which in turn improves stand mechanical stability and productivity (Ostendorp, 1999) while doing nothing to decrease competitive abilities (Mook & van der Toorn, 1982). The rapid invasion of common reed post-fire inhibits the recolonization of the pre-disturbance vegetation communities and, critically, increases vulnerability to future and repeated fires as it is highly flammable (Thompson & Shay, 1985). In contrast, a study in a Japanese marsh found that high-severity burns in common reed stands allowed for greater regeneration of other species from the seedbank, thereby limiting the return of common reed (Kimura & Tsuyuzaki, 2011). However, the fires in that study were non-peat consuming. Root burns have been shown to reduce the

growing ability of common reed where they occur but may not limit recolonization post-fire (Marks et al. 1994). Still, we believe that findings from the literature and those from this study provide credence to the hypothesis that common reed may be akin to other invasive grass species that can initiate and perpetuate positive grass-fire feedbacks (sensu D'Antonio & Vitousek, 1992), with impacts to carbon emissions and wetland habitat (Fig. 18).

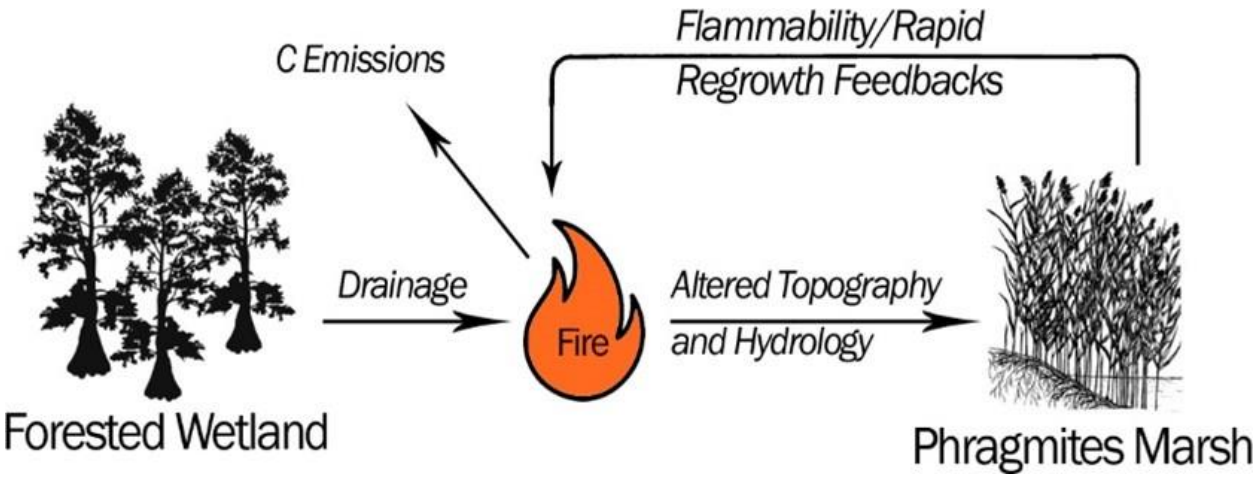

Figure 18: Proposed Phragmites-fire feedback. High-severity, peat-consuming fires, driven by a history of drainage, alter topography and therefore hydrology. The post-disturbance environment is primed for common reed invasion with wetter conditions and the aggressive nature of common reed allows it to outcompete other species. Other studies have shown that fires increase reed bud development and shoot density (Cowie et al., 1992; Ostendorp, 1999), and that stands are highly flammable (Thompson & Shay, 1985), so they may serve as future ignition points, thereby initiating a perpetual Phragmites-fire feedback cycle.

3.4.3 Limitations and Future Work

A major limitation to this study was the herbicide prescription applied to the management units south of Interior Ditch. The aerial application of herbicide is assumed to be responsible for the smaller proportion of common reed observations in those management units (18.30% of observations were common reed in our study management unit compared to 1.99% in all other management units). The exact boundaries of the herbicide treatment are unclear due to both the application method and the metadata associated with the prescription (Fig. A-2), which prevented us from including herbicide effects as another independent factor influencing common

reed occurrence. Thus, it limited our direct assessment of herbicide effectiveness and removed a sizeable amount of potential study area within the Lateral West burn scar.

We also chose not to include two other potential controls, nutrient gradients and distance to competitors, in our auto-logistic regression models. While nutrient patterns have been shown to impact common reed distributions (Long et al., 2017), they likely do not exist in our system as the area of interest is not neighboring agricultural runoff, the management units are hydrologically isolated, and GDS is largely a precipitation-fed system. We did not include distance to competitors because of the lower accuracy scores for both cattail and wool grass from our supervised classification (Table 2). Many of the ground-truthing points for these two classes were as pure as we could find but were less monotypic and smaller than the common reed observations, likely explaining their lower accuracy scores. Competitive interactions have been shown to be important in other ecosystems (Páramo Pérez et al., 2018; Shay et al., 1999) and may have exerted additional influence on common reed occurrence in our study area. Nonetheless, we note that hydrology has been shown to be the key factor controlling common reed distributions (Rohal et al., 2019) and that this study was primarily focused on the influence of disturbance-altered hydrology.

An interesting direction for future work would be to track common reed expansion over time following deep-smoldering fires. Using imagery of a single site across multiple seasons, a study of this nature could investigate the roles that disturbance-altered hydrology and other site factors play in governing the rate and direction of common reed colony expansion. Such work in our study management unit, however, would have to also consider the role of herbicide in common reed expansion (or contraction) as the area was treated soon after our satellite imagery was collected. An additional interesting avenue for future studies would be to intentionally test

the proposed Phragmites-fire feedback (Fig. 18). If common reed locations are identified both before and after a high severity fire, the change in common reed coverage could be easily assessed and compared between periods. This may require multiple rounds of ground-truthing data points to be collected as spectral properties may differ soon after fire (Pereira et al., 1999). Additionally, this analysis would rely on the occurrence of high-severity peat burns ,which are rare and intentionally prevented. Regardless, rigorous evaluation of the proposed Phragmites-fire feedback cycle in multiple systems and under multiple fire conditions is warranted and would inform both disturbance ecology and on-the-ground management efforts.

3.5 LITERATURE CITED

Able, K. W., & Hagan, S. M. (2003). Impact of common reed, *Phragmites australis*, on essential fish habitat: Influence on reproduction, embryological development, and larval abundance of mummichog (*Fundulus heteroclitus*). Estuaries 26: 40–50. https://doi.org/10.1007/BF02691692

Allouche, O., Tsoar, A., & Kadmon, R. (2006). Assessing the accuracy of species distribution models: Prevalence, kappa and the true skill statistic (TSS). Journal of Applied Ecology 43: 1223–1232. https://doi.org/10.1111/j.1365-2664.2006.01214.x

Amsberry, L., Baker, M. A., Ewanchuk, P. J., & Bertness, M. D. (2000). Clonal integration and the expansion of *Phragmites australis*. Ecological Applications, 10: 1110–1118. https://doi.org/10.1890/1051-0761(2000)010[1110:CIATEO]2.0.CO;2

Bart, D., & Hartman, J. M. (2003). The role of large rhizome dispersal and low salinity windows in the establishment of common reed, *Phragmites australis*, in salt marshes: New links to human activities. Estuaries 26: 436–443. https://doi.org/10.1007/BF02823720

Breiman, L. (2001). Statistical modeling: The two cultures. Statistical Science 16: 199–215. https://doi.org/10.1214/ss/1009213726

Chimner, R. A., Cooper, D. J., Wurster, F. C., & Rochefort, L. (2016). An overview of peatland restoration in North America: where are we after 25 years? Restoration Ecology 25: 283–292. https://doi.org/10.1111/rec.12434

Cowie, N. R., Sutherland, W. J., Ditlhogo, M. K. M., & James, R. (1992). The effects of conservation management of reed beds. II. The flora and litter disappearance. The Journal of Applied Ecology 29: 277-284. https://doi.org/10.2307/2404496

Cutler, D. R., Edwards, T. C., Beard, K. H., Cutler, A., Hess, K. T., Gibson, J., & Lawler, J. J. (2007). Random forests for classification in ecology. Ecology 88: 2783–2792. https://doi.org/10.1890/07-0539.1

D'Antonio, C. M., & Vitousek, P. M. (1992). Biological invasions by exotic grasses, the grass/fire cycle, and global change. Annual Review of Ecology and Systematics 23: 63–87. https://doi.org/10.1146/annurev.es.23.110192.000431

Davis, F. W., Stine, P. A., Stoms, D. M., Borchert, M. I., & Hollander, A. D. (1995). Gap analysis of the actual vegetation of California 1. The Southwestern Region. Madrono, 42: 40–78. Retrieved from https://www.jstor.org/stable/41425046?casa_token=SuajnfpjVOkAAAAA:xaXZcxz3bjge5gICyW-orL-6mkbutGe09G5z5GU_mNUq17K9P3pZKIlOG6GcLmFQg9xNK7SFI6CVWMFov2hOBI23v8yZGfzvuiLz4bnRRYPPyBeyfcg

Dix, M. E., Buford, M., Slavicek, J., Solomon, A. M., & Conard, S. G. (2010). Invasive species and disturbances: Current and future roles of forest service research and development. A Dynamic Invasive Species Research Vision: Opportunities and Priorities 29: 91-102

Evans, J., & Murphy, M. (2021). spatialEco. Retrieved from https://github.com/jeffreyevans/spatialEco

Farnsworth, E. J., & Meyerson, L. A. (1999). Species composition and inter-annual dynamics of a freshwater tidal plant community following removal of the invasive grass, *Phragmites australis*. Biological Invasions 1: 115–127. https://doi.org/10.1023/A:1010068607630

Flannigan, M., Stocks, B., Turetsky, M., & Wotton, M. (2009). Impacts of climate change on fire activity and fire management in the circumboreal forest. Global Change Biology 1: 549–560. https://doi.org/10.1111/j.1365-2486.2008.01660.x

Gorham, E., & Rochefort, L. (2003). Peatland restoration: A brief assessment with special reference to sphagnum bogs. Wetlands Ecology and Management 11: 109–119. https://doi.org/10.1023/A:1022065723511

Haslam, S. M. (1972). *Phragmites Communis Trin . (Arundo Phragmites L .,? Phragmites Australis* (Cav .) Trin . ex Steudel. Journal of Ecology 60: 585–610.

Hellings, S. E., & Gallagher, J. L. (1992). The Effects of Salinity and Flooding on *Phragmites australis*. The Journal of Applied Ecology 29: 41–49. https://doi.org/10.2307/2404345

Hudon, C., Gagnon, P., & Jean, M. (2005). Hydrological factors controlling the spread of common reed (*Phragmites australis*) in the St. Lawrence River (Québec, Canada). Ecoscience 12: 347–357. https://doi.org/10.2980/i1195-6860-12-3-347.1

Hutchinson, G. . (1967). A Treatise on limnology: Introduction to lake biology and the limnoplankton. John Wiley & Sons, New York, London, and Sydney (Vol. 2). https://doi.org/10.4319/lo.1969.14.3.0472

Ji, Y. H., Zhou, G. S., Lv, G. H., Zhao, X. L., & Jia, Q. Y. (2009). Expansion of *Phragmites australis* in the Liaohe Delta, north-east China. Weed Research 49: 613–620. https://doi.org/10.1111/j.1365-3180.2009.00727.x

Kercher, S. M., Carpenter, Q. J., & Zedler, J. B. (2004). Interrelationships of hydrologic disturbance, reed canary grass (*Phalaris arundinacea L.*), and native plants in Wisconsin wet meadows. Natural Areas Journal 24: 316–325.

Kettenring, K. M., & Mock, K. E. (2012). Genetic diversity, reproductive mode, and dispersal differ between the cryptic invader, *Phragmites australis*, and its native conspecific. Biological Invasions 14: 2489–2504. https://doi.org/10.1007/s10530-012-0246-5

Kettridge, N., Turetsky, M. R., Sherwood, J. H., Thompson, D. K., Miller, C. A., Benscoter, B. W., … Waddington, J. M. (2015). Moderate drop in water table increases peatland vulnerability to post-fire regime shift. Scientific Reports 5:1-4. https://doi.org/10.1038/srep08063

Kimura, H., & Tsuyuzaki, S. (2011). Fire severity affects vegetation and seed bank in a wetland. Applied Vegetation Science 14: 350–357. https://doi.org/10.1111/j.1654-109X.2011.01126.x

L3Harris Geospatial. (2022). Vegetation indices. https://www.l3harrisgeospatial.com/docs/vegetationindices.html

Lane, C. R., Liu, H., Autrey, B. C., Anenkhonov, O. A., Chepinoga, V. V., & Wu, Q. (2014). Improved wetland classification using eight-band high resolution satellite imagery and a hybrid approach. Remote Sensing 6: 12187–12216. https://doi.org/10.3390/rs61212187

Liaw, A., & Wiener, M. (2002). Classification and Regression by randomForest. R News 2: 18–22.

Libby, N., Perry, J. E., & Haven, K. J. (2002). A summary of methods for controlling *Phragmites australis*. Gloucester Point, VA. Retrieved from https://catalog.lib.vt.edu/cgi-bin/koha/opac-detail.pl?biblionumber=473747

Long, A. L., Kettenring, K. M., Hawkins, C. P., & Neale, C. M. U. (2017). Distribution and drivers of a widespread, invasive wetland grass, *Phragmites australis*, in wetlands of the Great Salt Lake, Utah, USA. Wetlands 37: 45–57. https://doi.org/10.1007/s13157-016-0838-4

Loveless, C. M. (1959). A study of the vegetation in the Florida everglades. Ecology 40: 1–9. https://doi.org/10.2307/1929916

Ludwig, R. F., McLaughlin, D. L., & Wurster, F. C. (2021). Red maple dominance and community homogenization in a disturbed forested wetland. Wetlands Ecology and Management 29: 599–615. https://doi.org/10.1007/s11273-021-09808-6

MacDougall, A. S., & Turkington, R. (2005). Are invasive species the drivers or passengers of change in degraded ecosystems? Ecology 86: 42–55. https://doi.org/10.1890/04-0669

Maheu-Giroux, M., & De Blois, S. (2007). Landscape ecology of *Phragmites australis* invasion in networks of linear wetlands. Landscape Ecology 22: 285–301. https://doi.org/10.1007/s10980-006-9024-z

Mal, T. K., & Narine, L. (2003). The biology of Canadian weeds. 129. *Phragmites australis* (Cav.) Trin. ex Steud. Canadian Journal of Plant Science 84: 365–396. https://doi.org/10.4141/P01-172

Marks, M., Lapin, B., & Randall John. (1994). *Phragmites australis* (*P. communis*): Threats, management, and monitoring. Natural Areas Journal 14: 185–194. Retrieved from http://www.naturalareas.org/docs/66NAJ1404_285-294.pdf

Matlaga, D. P., Quintana-Ascencio, P. F., Menges, E. S., & Pickert, R. (2010). Fire mediated edge effects in bayhead tree islands. Journal of Vegetation Science 21: 190–200. https://doi.org/10.1111/j.1654-1103.2009.01132.x

Mook, J. H., & van der Toorn, J. (1982). The influence of environmental factors and management on stands of *Phragmites australis* II. effects on yield and its relationships with shoot density. Journal of Applied Ecology 19: 501–517.

Moran, P. A. P. (1950). Notes on continuous stochastic phenomena. Biometrika 37: 17-23. https://doi.org/10.2307/2332142

NASA. (2022). Fire in Great Dismal Swamp, Virginia. Retrieved from https://earthobservatory.nasa.gov/images/51670/fire-in-great-dismal-swamp-virginia

Ostendorp, W. (1999). Management impacts on stand structure of lakeshore *Phragmites reeds*. International Review of Hydrobiology 84: 33–47. https://doi.org/10.1002/iroh.199900006

Page, S., & Baird, A. J. (2016). Peatlands and global change: Response and resilience. Annual Review of Environment and Resources 41: 35–57. https://doi.org/10.1146/annurev-environ-110615-085520

Page, S., Hosciło, A., Wösten, H., Jauhiainen, J., Silvius, M., Rieley, J., … Limin, S. (2009). Restoration ecology of lowland tropical peatlands in Southeast Asia: Current knowledge and future research directions. Ecosystems 12: 888–905. https://doi.org/10.1007/s10021-008-9216-2

Páramo Pérez, M. E., Lindig-Cisneros, R., & Moreno-Casasola, P. (2018). Invasiveness of *Phragmites australis* in communities dominated by native species after fire disturbance under controlled conditions. Hidrobiologica 28: 201–207. https://doi.org/10.24275/uam/izt/dcbs/hidro/2018v28n2/lindig

Parthum, B., Pindilli, E., & Hogan, D. (2017). Benefits of the fire mitigation ecosystem service in The Great Dismal Swamp National Wildlife Refuge, Virginia, USA. Journal of Environmental Management 203: 375–382. https://doi.org/10.1016/j.jenvman.2017.08.018

Pereira, J. M. C., Sá, A. C. L., Sousa, A. M. O., Silva, J. M. N., Santos, T. N., & Carreiras, J. M. B. (1999). Spectral characterisation and discrimination of burnt areas. In Remote Sensing of Large Wildfires (pp. 123–138). Springer Berlin Heidelberg. https://doi.org/10.1007/978-3-642-60164-4_7

Poulter, B., Christensen, N. L., & Halpin, P. N. (2006). Carbon emissions from a temperate peat fire and its relevance to interannual variability of trace atmospheric greenhouse gases. Journal of Geophysical Research 111: 1-11. https://doi.org/10.1029/2005JD006455

Qi, Y. (2012). Random forest for bioinformatics. Ensemble Machine Learning (pp. 307–323). Springer Boston Massachusetts . https://doi.org/10.1007/978-1-4419-9326-7_11

R Core Team. (2020). R: a language and environment for statistical computing. R Foundation for Statistical Computing. Vienna, Austria.

Rea, N. (1996). Water levels and Phragmites: Decline from lack of regeneration or dieback from shoot death. Folia Geobotanica 31: 85–90. https://doi.org/10.1007/bf02803997

Reddy, A. D., Hawbaker, T. J., Wurster, F., Zhu, Z., Ward, S., Newcomb, D., & Murray, R. (2015). Quantifying soil carbon loss and uncertainty from a peatland wildfire using multi-temporal LiDAR. Remote Sensing of Environment 170: 306–316. https://doi.org/10.1016/j.rse.2015.09.017

Refaeilzadeh, P., Tang, L., & Liu, H. (2016). Cross-Validation. Encyclopedia of Database Systems (pp. 1–7). https://doi.org/10.1007/978-1-4899-7993-3_565-2

Rein, G. (2015). Chapter 1 - smoldering-peat megafires: The largest fires on earth. Coal and Peat Fires: a Global Perspective 4: 1-11. https://doi.org/10.1016/B978-0-444-59510-2.00001-X

Robichaud, C. D., & Rooney, R. C. (2017). Long-term effects of a *Phragmites australis* invasion on birds in a Lake Erie coastal marsh. Journal of Great Lakes Research 43: 141–149. https://doi.org/10.1016/j.jglr.2017.03.018

Rohal, C. B., Cranney, C., Hazelton, E. L. G., & Kettenring, K. M. (2019). Invasive *Phragmites australis* management outcomes and native plant recovery are context dependent. Ecology and Evolution 9: 13835–13849. https://doi.org/10.1002/ece3.5820

Rolletschek, H., Hartzendorf, T., Rolletschek, A., & Kohl, J. G. (1999). Biometric variation in *Phragmites australis* affecting convective ventilation and amino acid metabolism. Aquatic Botany 64: 291–302. https://doi.org/10.1016/S0304-3770(99)00057-1

Shay, J. M., De Geus, P. M. J., & Kapinga, M. R. M. (1999). Changes in shoreline vegetation over a 50-year period in the Delta Marsh, Manitoba in response to water levels. Wetlands 19: 413–425. https://doi.org/10.1007/BF03161773

Turetsky, M. R., Benscoter, B., Page, S., Rein, G., Van Der Werf, G. R., & Watts, A. (2015). Global vulnerability of peatlands to fire and carbon loss. Nature Geoscience 8: 11–14. https://doi.org/10.1038/ngeo2325

USFWS. (2006). Great Dismal Swamp National Wildlife Refuge and Nansemond National Wildlife Refuge final comprehensive conservation plan July 2006. USFWS.

Usup, A., Hashimoto, Y., Takahashi, H., & Hayasaka, H. (2004). Combustion and thermal characteristics of peat fire in tropical peatland in Central Kalimantan, Indonesia. Tropics, 14: 1–19. https://doi.org/10.3759/tropics.14.1

van der Valk, A. G. (1994). Effects of prolonged flooding on the distribution and biomass of emergent species along a freshwater wetland coenocline. Vegetatio 110: 185–196. https://doi.org/10.1007/BF00033398

Ward, P. (1968). Fire in relation to waterfowl habitat of the delta marshes. 8th Tall Timbers Fire Ecology Conference: 255–267

Watts, A. C., & Kobziar, L. N. (2013). Smoldering combustion and ground fires: Ecological effects and multi-scale significance. Fire Ecology 9: 124–132. https://doi.org/10.4996/fireecology.0901124

Watts, A. C., Schmidt, C. A., McLaughlin, D. L., & Kaplan, D. A. (2015). Hydrologic implications of smoldering fires in wetland landscapes. Freshwater Science 34: 1394–1405. https://doi.org/10.1086/683484

Weisner, S. E. B., Graneli, W., & Ekstam, B. (1993). Influence of submergence on growth of seedlings of *Scirpus lacustris* and *Phragmites australis*. Freshwater Biology 29: 371–375. https://doi.org/10.1111/j.1365-2427.1993.tb00771.x

Wilcox, K. L., Petrie, S. A., Maynard, L. A., & Meyer, S. W. (2003). Historical distribution and abundance of *Phragmites australis* at Long Point, Lake Erie, Ontario. Journal of Great Lakes Research 29: 664–680. https://doi.org/10.1016/S0380-1330(03)70469-9

Zedler, J. B., & Kercher, S. (2004). Causes and consequences of invasive plants in wetlands: Opportunities, opportunists, and outcomes. Critical Reviews in Plant Sciences 23: 431-452. https://doi.org/10.1080/07352680490514673

4.0 CONCLUSIONS

The overall objective of this work was to investigate the drivers and impacts of smoldering peat fires in a drained temperate peatland, the Great Dismal Swamp (GDS) (Fig.1). We first sought to develop a new method for modeling smoldering depths in organic soils (Chapter 2) and then studied the impact of such fires on the distribution of an invasive grass (Chapter 3). These two complimentary goals were built upon prior studies and in-field observations and were aimed to answer important questions posed by land managers. Employing a variety of research techniques and data types, we were able to speak to both causes and consequences of high severity peat fires. Our results, therefore, may be used to inform peatland management strategies for prioritizing wildfire prevention and post-burn restoration.

In the first study (Chapter 2), we developed and verified a simple approach to model potential burn depths in organic soils. Assuming a state of hydrostatic equilibrium, our method worked by combining peat hydraulic property data and water table observations with moisture-to-ignition thresholds. We compared modeled moisture regimes and modeled burn depths from the process-based model HYDRUS against those from this simpler, water table-based approach to evaluate its outputs and test its necessary assumptions. The results from this comparison demonstrated that the water table-based method made similar burn depth predictions, especially in low water retention peats (Table 1). As many of the upper layer peats in GDS have poor water retention properties (Fig. 2), we applied this approach to 11 spatially distributed sites across our study area (Fig. 1) for a 2.5-year period of water table record (Fig. 5). The comparison of burn depth predictions between sites indicated that contemporaneous water levels primarily govern fire risk, but that peat water retention properties also exert a degree of influence (Fig. 8). However, there was a strong, significant relationship between these two factors which indicates

that drainage may weaken both short- and long-term controls of smoldering burn depths and risk. Our results imply that drained peats may be constantly under threat of burning up to the water table, but also suggest that rewetting efforts may be an effective strategy to mitigate peatland wildfire risk.

In the second study (Chapter 3), we mapped the distribution of *Phragmites australis* (common reed) in a portion of the 2,500 ha burn scar in GDS (Fig. 14). We aimed to relate its occurrence and coverage to site factors, with special focus on hydrology – which was shaped by two recent, deep smoldering wildfires. We hypothesized that common reed would be found in sites that are often shallowly flooded and that higher levels of common reed coverage would be related to more specific hydrologic windows. Further, we explored the potential connection between ideal hydrologic setting for common reed and the site history of drainage and bathymetry-altering peat fires. Through the use of high-resolution satellite imagery, machine learning algorithms, LiDAR data, and water table observations, we were able to conduct a number of analyses to investigate our hypotheses. Our results confirmed the notion that there was a relationship between common reed coverage and hydrology (Fig. 15), and found that the influence of spatial autocorrelation, while important at fine resolutions, was supplanted by hydrology at larger spatial scales (Table 3). Interestingly, we found that sites that had been burned twice, once in 2008 and again in 2011, were wetter on average than sites that had burnt once (Fig. 17). These sites, likely because of the increased burning, had a hydrology more suited to high common reed coverage and we found more common reed observations in them (Fig. 16). While these correlations do not explain the causal pathway on their own, we do point to the grass-fire feedback cycle that has been well demonstrated in other ecosystems. The competitive advantages of common reed, its life history, and its flammability further support this hypothesis.

We emphasize here that while this observational study merely draws a correlation between common reed coverage and a disturbance-altered hydrology, we feel that rigorous experimentation is warranted to test the potential for Phragmites-fire feedbacks (Fig. 18).

Our results from these two studies implicate the history of drainage at GDS for causing multiple, connected ecological issues. Drainage reduced both the short- and long-term controls on deep smoldering fires (Fig. 8), which degraded the ecosystem's resilience and generated a hydrology ideal for the invasion of common reed. There is reasonable concern that common reed colonies may perpetuate grass-fire feedbacks, thereby amplifying the increased fire risk and subsequent susceptibility to invasives (Fig 18). Our findings add to the general body of literature on disturbances and invasive species in peatlands. Further, our results may help land managers at GDS and other similar peatlands reduce their risk to wildfires and species invasions. In short, these studies underscore the overarching influence that water levels have in peatlands on everything from community makeup to disturbance regimes. Said another way, and to loosely borrow from prominent wetland ecologist Paul A. Keddy: it's the hydrology, stupid.

5.0 APPENDIX

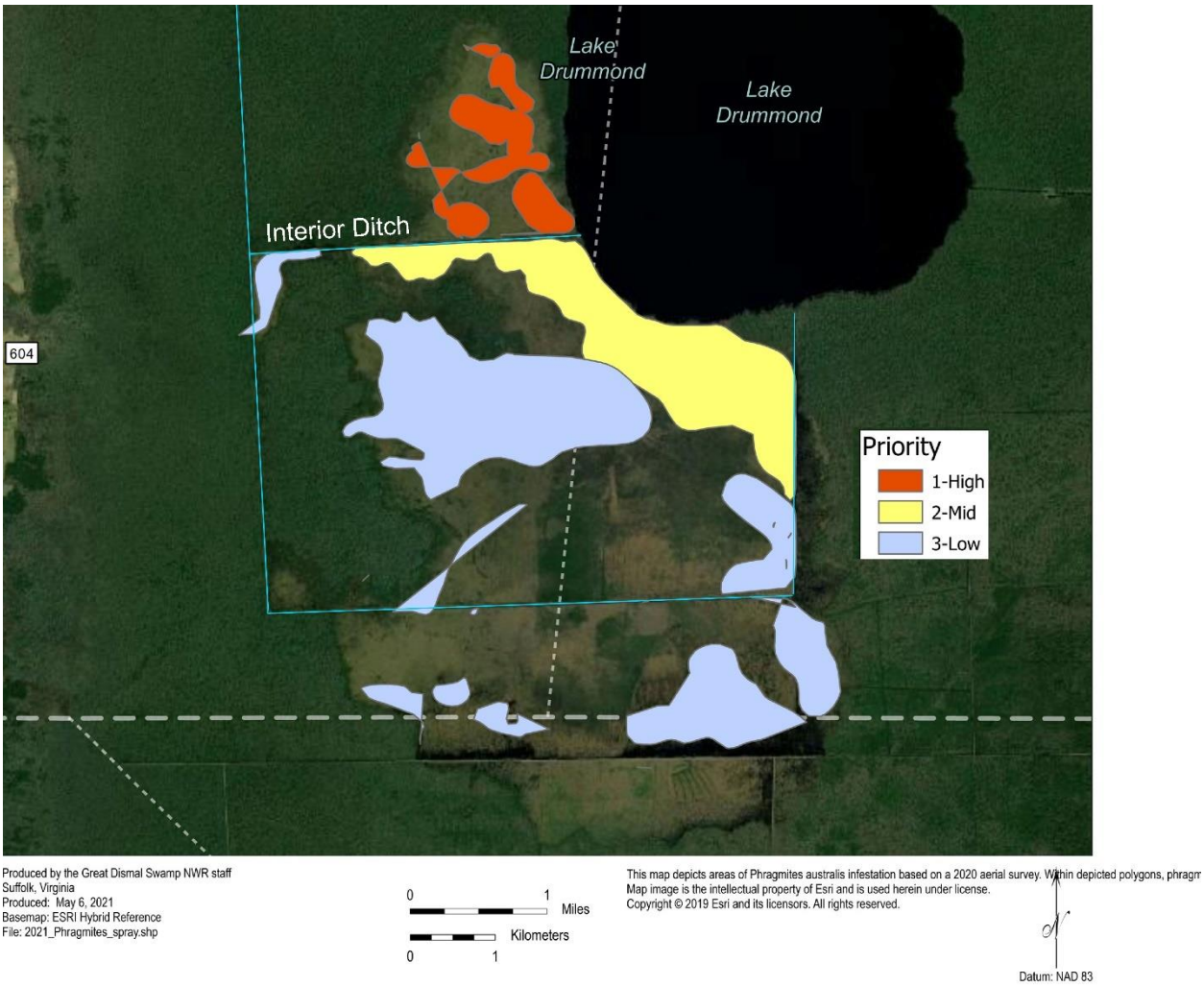

Figure A-1: *Phragmites australis* observations from a 2020 aerial survey, conducted by the US Fish and Wildlife Service. Figure courtesy of the Great Dismal Swamp National Wildlife Refuge staff of the US Fish and Wildlife Service.

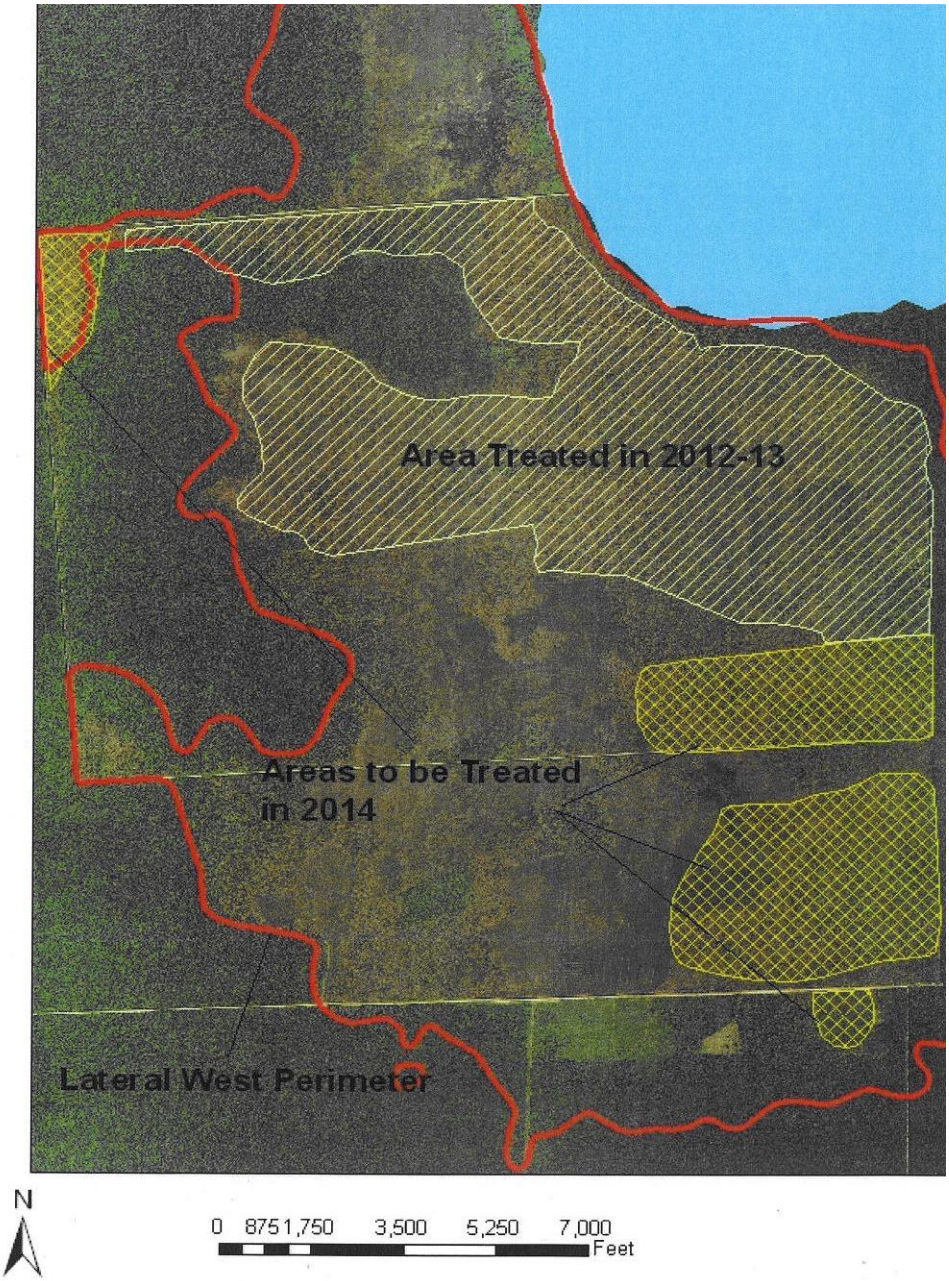

Figure A-2: Great Dismal Swamp National Wildlife Refuge *Phragmites australis* treatment areas 2012-2013. Lateral West burn scar perimeter noted in red. Figure courtesy of the Great Dismal Swamp National Wildlife Refuge staff of the US Fish and Wildlife Service.

Table A-1: List of the forty-four spectral indices calculated from the 8-band WorldView-2 satellite image. These index values were used in the random forest modeling for land cover identification. B1 = Coastal Blue, B2 = Blue, B3 = Green, B4 = Yellow, B5 = Red, B6 = Red Edge, B7 = NIR, B8 = NIR2.

Spectral Index	Description
ARVI	Atmospherically Resistant Vegetation Index (B7-(2*B5)+B3)/(B7+(2*B5)+B3)
CCCI	Canopy Chlorophyll Content Index [(B8-B6)/(B8+B6)]/[(B8-B5)/(B8+B5)]
EVI	Enhanced Vegetation Index 2.5 * (B7-B5)/(B7+6*B5-7.5*B2+1)
GNDVI	Green Normalized Difference Vegetation Index (B7-B3)/(B7+B3)
MCARI	Modified Chlorophyll Absorption Ratio Index [(B6-B5)-0.2(B6-B3)]*(B6/B5)
MRESRI	Modified Red Edge Simple Ratio Index (B6/B5)-1/(SQRT(B6/B5))+1
MSAVI2	Modified Soil Adjusted Vegetation Index 2 2*B7+1-SQRT((2*B7+1)^2-8(B7-B5))/2
MSRI1	Modified simple Ratio Index 1 (B7/B5)-1/(SQRT(B7/B5))+1
MSRI2	Modified simple Ratio Index 2 (B8/B5)-1/(SQRT(B8/B5))+1
MTCI	MERIS Terrestrial Chlorophyll Index (B7-B6)/(B6-B5)
NDMI	Normalized Difference Moisture Index B7-B8/B7+B8
NDVI75	Normalized Difference Vegetation Index 75 B7-B5/B7+B5
NDVI85	Normalized Difference Vegetation Index 85 B8-B5/B8+B5

OSAVI	Optimized Soil Adjusted Vegetation Index (B7-B5)/(B7+B5+1.6)
RDVI	Renormalized Difference Vegetation Index (B7-B5)/SQRT(B7+B5)
RECI	Red Edge Chlorophyll Index (B7/B6)-1
RENDVI	Red Edge Normalized Difference Vegetation Index B6-B5/B6+B5
RESRI	Red Edge Simple Ratio Index B6/B5
SAVI	Soil Adjusted Vegetation Index 1.5*(B7-B5)/(B7+B5+0.5)
SIPI	Structure Insensitive Pigment Index B7-B1/B7-B5
SR1	Simple Ratio 1 B7/B5
SR2	Simple Ratio 2 B8/B5
TCARI	Transformed Chlorophyll Absorption Reflectance Index 3[(B6-B5)-0.2(B6-B3)(B6/B5)]
TVI	Triangular Vegetation Index 120(B6-B3)-200(B6-B3)/2
WDRVI	Wide Dynamic Range Vegetation Index (0.2*B7-B5)/(0.2*B7+B5)
WVSI	WorldView Soil Index B3-B4/B3+B4
WVWI	WorldView Water Index B1-B8/B1+B8
NIRV756	Near Infrared Vegetation Index NDVI75*B6

NIRV757	Near Infrared Vegetation Index NDVI75*B7
NIRV758	Near Infrared Vegetation Index NDVI75*B8
NIRV856	Near Infrared Vegetation Index NDVI85*B6
NIRV857	Near Infrared Vegetation Index NDVI85*B7
NIRV858	Near Infrared Vegetation Index NDVI85*B8
REVI6	RENDVI*B6
REVI7	RENDVI*B7
REVI8	RENDVI*B8
PCA_1	Principal Component Analysis Band 1
PCA_2	Principal Component Analysis Band 2
PCA_3	Principal Component Analysis Band 3
PCA_4	Principal Component Analysis Band 4
PCA_5	Principal Component Analysis Band 5
PCA_6	Principal Component Analysis Band 6
PCA_7	Principal Component Analysis Band 7
PCA_8	Principal Component Analysis Band 8